CHINESE JOURNAL OF PHYSICS

ISSN: 0577-9073; Impact factor = 2.638; Publisher - Elsevier

Accepted September 16th 2020

Modeling the onset of thermosolutal convective instability in a non-Newtonian nanofluid-saturated porous medium layer

J.C. Umavathi[1*] and **O. Anwar Bég[2]**

[1]Professor of Applied Mathematics, Department of Mathematics, Gulbarga University, Gulbarga-585 106, Karnataka, ***INDIA***

[2]Professor of Engineering Science & Director Multi-Physical Engineering Sciences Group (MPESG), Department of Aeronautical/Mechanical Engineering, School of Science, Engineering and Environment (SEE), University of Salford, Manchester, M5 4WT, ***UK.***

****Corresponding author*** ***Email: drumavathi@rediffmail.com***

ABSTRACT

The onset of double-diffusive (thermosolutal) convection in horizontal porous layer saturated with an incompressible couple stress nanofluid saturated is studied with thermal conductivity and viscosity dependent on the nanoparticle volume fraction. To represent the momentum equation for porous media, a modified Darcy-Maxwell nanofluid model incorporating the effects of Brownian motion and thermophoresis has been used. The thermal energy equation includes regular diffusion and cross diffusion (Soret thermo-diffusion and Dufour diffuso-thermal) terms. A linear stability analysis depends on the normal mode technique and the onset criterion for stationary and oscillatory convection is derived analytically. The nonlinear theory based on the representation of the Fourier series method is applied to capture the behavior of heat and mass transfer. It is found that the couple stress parameter enhances the stability of the system in both the stationary and oscillatory convection modes. The viscosity ratio and conductivity ratio both enhance heat and mass transfer. Transient Nusselt number is found to be oscillatory when time is small. However, when time becomes very large, all the three transient Nusselt number values approach to their steady state values.

keywords: Nanofluid, Couple stress rheology, Soret parameter, Dufour parameter, Brownian motion, Thermophoresis.

Nomenclature

C	solute concentration (moles)
D_B	Brownian diffusion coefficient (m^2/s)
D_T	thermophoretic diffusion coefficient (m^2/s)
H	dimensional sandwich layer depth (m)
k	thermal conductivity of the nanofluid ($W/m\,K$)
k_m	overall thermal conductivity of the porous medium saturated by the nanofluid ($W/m\,K$)
K	permeability (m^2)
Le	thermo-solutal Lewis number
Ln	Lewis number
N_A	modified diffusivity ratio
N_B	modified particle-density increment
N_{CT}	Soret parameter
N_{TC}	Dufour parameter
p^*	pressure (Pa)
p	dimensionless pressure, $\left(p^*K\right)/\left(\mu\alpha_f\right)$
γ_a	non dimensional acceleration coefficient
Va	Vadász number
Ra_T	thermal Rayleigh- Darcy number
Rm	basic-density Rayleigh number
Rn	concentration Rayleigh number
C_P	Couple-stress parameter, $\frac{\mu_C}{\mu_{eff}\,H^2}$
Rs	solutal Rayleigh number
t^*	time (s)
t	dimensionless time, $\left(t^*\alpha_f\right)/H^2$
T^*	nanofluid temperature (K)

T	dimensionless temperature, $\frac{T^* - T_c^*}{T_h^* - T_c^*}$
T_c^*	temperature at the upper wall (K)
T_h^*	temperature at the lower wall (K)
(u, v, w)	dimensionless Darcy velocity components $\left(u^*, v^*, w^*\right) H/\alpha_m$ (m/s)
$\mathbf{v}$	nanofluid velocity (m/s)
(x, y, z)	dimensionless Cartesian coordinate $\left(x^*, y^*, z^*\right)/H$; z is the vertically upward coordinate
$\left(x^*, y^*, z^*\right)$	Cartesian coordinates

Greek symbols

α_f	thermal diffusivity of the fluid, (m/s^2)
β_C	solutal volumetric coefficient (K^{-1})
β_T	thermal volumetric coefficient (K^{-1})
ν	viscosity variation parameter
ε	porosity
η	thermal conductivity variation parameter
μ	dynamic viscosity of the fluid (kgm/s)
ρ	fluid density (kg/m^3)
ρ_p	nanoparticle mass density (kg/m^3)
σ	thermal capacity ratio
ϕ^*	nanoparticle volume fraction
ϕ	relative nanoparticle volume fraction, $\frac{\phi^* - \phi_0^*}{\phi_1^* - \phi_0^*}$

Subscripts/superscripts

b	basic solution
f	fluid
p	particle

*	dimensional variable
'	perturbed variable
St	stationary
Osc	oscillatory

1. Introduction

A fluid that contains particles with dimensions less than 100 nm is referred to as a nanofluid. The base fluid, or dispersing medium, can be aqueous or non-aqueous in nature. Typical nanometer-sized particles are metals, oxides, carbides, nitrides or carbon nanotubes. Their shapes may be spheres, discs or rods. Since nanofluids offer significant potential applications in engineering (e.g. petroleum recovery, electronics cooling etc), hence the study of nanofluids has evolved into a substantial branch of nanotechnology. The fundamental science of nanofluids spans colloidal science, surface chemistry, fluid mechanics and materials science. There has been a significant interest in nanofluids in recent years. This interest is generated by a variety of applications, ranging from laser-assisted drug delivery to heating control in lubrication systems. Nanofluids are composed of nanoparticles (with sizes typically in the range between 1 and 100 nm) suspended in a base fluid, which can be water or an organic solvent [1,2]. The area of nanofluids was pioneered by Choi and Eastman [3]. Characteristic features of nanofluids are the formation of very stable colloidal systems with very little settling (the stability of the suspension is typically achieved by electrostatic stabilization by adjusting the pH, [4]) and anomalous enhancement of the thermal conductivity in comparison with the base fluid [5]. An extensive number of recent papers report on the experimental measurements of thermophysical properties of nanofluids, including specific heat, thermal conductivity and viscosity [6-8]. Lee et al. [9] Researchers have demonstrated that oxide ceramic nanofluids consisting of CuO or Al_2O_3 nanoparticles in water or EG exhibit enhanced thermal conductivity. Theoretical work for the nanofluids in the framework of boundary layer theory was initiated by Buongiorno [10] by emphasizing the Brownian diffusion and thermophoresis slip mechanisms; this became subsequently known as the “Buongiorno model” and set a benchmark among later nanofluid boundary layer modelling. Combined thermophoresis and Brownian motion effects on nanofuid free convection heat transfer in an L-shaped enclosure were taken into consideration by Sheikholeslami *et al.* [11]. Their results show that the Nusselt number increases with

increases in either the thermal Rayleigh number or the Lewis number whereas it decreases with increases in either the aspect ratio or concentration Rayleigh number.

The unsteady stagnation-point flow and heat transfer of a nanofluid containing gyrotactic microorganisms past a permeable moving surface was researched by Basir *et al.* [12]. They concluded that stability analysis distinguishes the upper branch solution as a stable solution, whereas the lower solution is the unstable solution. Sheikholeslami *et al.* [13] demonstrated experimentally the influence of adding nanoparticles in boiling heat transfer of R600a within flattened pipes. They used R600a/oil/Cuo as a carrier fluid and they concluded that an increase in the flattened percentage enhances the heat transfer coefficient. The impact of using fins and nano-sized materials on performance of discharging systems was investigated by Sheikholeslami *et al.* [14]. They reported that the shapes of nanoparticles also effect the transient process and that the presence of nanoparticles improves the discharging rate. Recently Sheikholeslami *et al.* [15] studied methods for accelerating discharge process of clean energy storage unit with insertion of porous foam considering nanoparticles enhanced with paraffin. They noted that throughout solidification, liquid paraffin loses heat to air and become colder itself and solidifies and effectively this process guides the air to become warmer. Sheikholeslami *et al.* [16] scrutinized energy and entropy generation in a two-phase simulation of nanoparticles within a solar unit featuring a new turbulator. They claimed that to reach the accurate simulation of nanofluid, non-homogenous models give better results in comparison with single-phase models. Mahalakshmi *et al.* [17] investigated numerically the natural convection inside an enclosure with a centre heater using nanofluids. They considered Ag, CuO and Al_2O_3 as nanoparticles and water as the carrier fluid. They proved that heat transfer was elevated with the heater and higher Rayleigh numbers.

In recent years, a new type of heat transfer fluid using “hybrid nanofluids" has been developed. Different from the regular nanofluid which contains one type of nanoparticle, a hybrid nanofluid is an advanced nanofluid that contains two distinct nanoparticles dissolved in the base fluid. Waini *et al.* [18] derived and studied dual solutions of the unsteady flow of a hybrid nanofluid along a stretching or shrinking surface with heat transfer. Solution stability was analysed by conducting a temporal stability analysis, and it was shown that only one solution is stable whereas the other is not practicable. Waini *et al.* [19] also reported on

steady flow and heat transfer of hybrid nanofluids from a permeable moving surface. They used alumina and copper as nanoparticles and water as a carrier fluid. They discovered that the second solution was not stable while the first solution was stable. Izadia *et al.* [20] also considered hybrid nanofluids to investigate free convection under an inclined periodic magnetic field within a porous medium. They considered the nano-liquid as Ag-MgO nanosized particles inserted in water, observing that the magnetic field inclination angle and periodical magnetic field wavelength control the heat transfer performance within the liquid and solid phases.

One promising application of nanofluids is heat transfer enhancement, and there is still a considerable number of unanswered questions in this area. During the last few decades, the problem of double-diffusive (thermo-solutal) convection in porous media has attracted considerable interest. Such flows arise in a wide range of applications, from the solidification of binary mixtures to the migration of solutes in water-saturated soils. Geophysical systems, electrochemistry and the migration of moisture through air contained in fibrous insulation are some other important examples. A comprehensive review of the literature concerning double-diffusive natural convection in a fluid-saturated porous medium is provided by Nield and Bejan [21]. The articles by Mojtabi [22], Mojtabi and Charrier-Mojtabi [23] and Mamou [24] also furnish detailed surveys of double-diffusive convection in porous media. The multi-dimensional heat equation of arbitrary order which arises in the diffusion process was derived by Kumar *et al.* [25] using He's homotopy perturbation transform method and a residual power series method. A comparative study using Harr's wavelet and Adams-Bashforth-Moulton methods, was also presented by Kumar *et al.* [26] who studied the well-known Lotka-Bolterra population model. Mixed convective flow in a vertical channel filled with electrically conducting viscous fluid with isothermal wall conditions was investigated by Umavathi *et al.* [27] for variable fluid properties.

All the earlier studies on double-diffusive convective transport phenomena in porous media have been mainly concerned with the problem of convective instability in a horizontal layer heated with salt diffusion from below. Nield [28] initiated the study of double-diffusive convection in a porous medium based on linear stability theory for various thermal and solutal boundary conditions. An extension of Nield's analysis was reported by Taunton *et al.* [29] who examined the salt-fingering convection case in a porous layer. In modern

engineering technology, the importance of non-Newtonian fluids has been growing with the development of novel systems and products and hence the investigations on such fluids are desirable. During recent years the theory of microstructural fluids has received much attention since traditional Newtonian fluids cannot precisely describe the characteristics of fluids containing suspended particles. The study of such fluids finds applications in the extrusion of polymers, solidification of liquid crystals, cooling of metallic plates in a bath, exotic lubricants, geophysical convection and colloidal suspensions in chemical engineering. In the category of non-Newtonian fluids, couple stress fluid has distinct features, such as polar effects. The theory of polar fluids and related theories provide a sound framework for simulating liquids with significant microstructural characteristics. Couple stresses are of noticeable magnitude in liquids with very large molecules.

The thermal stability of a couple stress fluids has also received attention. Various investigators have considered multiple physical effects. Onset of thermal convection in an electrically conducting couple-stress fluid-saturated porous layer in the presence of a magnetic field was studied by Sharma and Thakur [30]. They reported that increasing couple stress effect postpones the onset of stationary convection. Sunil *et al.* [31] studied the hydrodynamic stability of superposed couple-stress fluids in a porous medium with magnetic body force. They derived a sufficient condition for the non-existence of over-stability. In another work, the effect of suspended particles on double-diffusive convection in a couple-stress fluid-saturated porous medium was investigated by Sunil *et al.* [32]. They reported that for the case of *stationary* convection, the stable solute gradient and couple stress have stabilizing effects, whereas the suspended particles and medium permeability have destabilizing effects.

Inspection of the scientific literature shows that the double diffusive (thermo-solutal) convection in a layer of porous medium saturated by a couple stress nanofluid however has not, thus far, received attention despite important applications in for example enhanced oil recovery. Therefore, the objective of the present paper is to investigate this problem in a parallel plate configuration with the additional effects of Soret and Dufour thermodiffusion and diffuso-thermal gradients, viscosity variation and thermal conductivity variation. Emphasis is placed on evaluating the onset of double diffusive convection using the couple stress non-Newtonian model with emphasis on how the conditions for the onset of

convection are modified by the presence of non-reactive, homogenously dispersed nanoparticles. Further we perform a weakly non-linear stability analysis of the rheological nanofluid thermal instability porous medium problem using the minimal representation of Fourier series to compute heat and mass transfer characteristics at the system boundaries (plates). Comprehensive visualization of computations is included, and a detailed interpretation provided.

2. Mathematical formulation

2.1 Conservation equations

We select a coordinate frame in which the z^*-axis is aligned vertically upwards. We consider a horizontal layer of couple stress nanofluid confined between the planes $z^* = 0$ and $z^* = H$. Asterisks are used to denote dimensional variables. Each boundary wall (plate) is assumed to be perfectly thermally conducting. The regime is depicted in **Fig. 1**. The plates lie in the x^*-y^* plane.

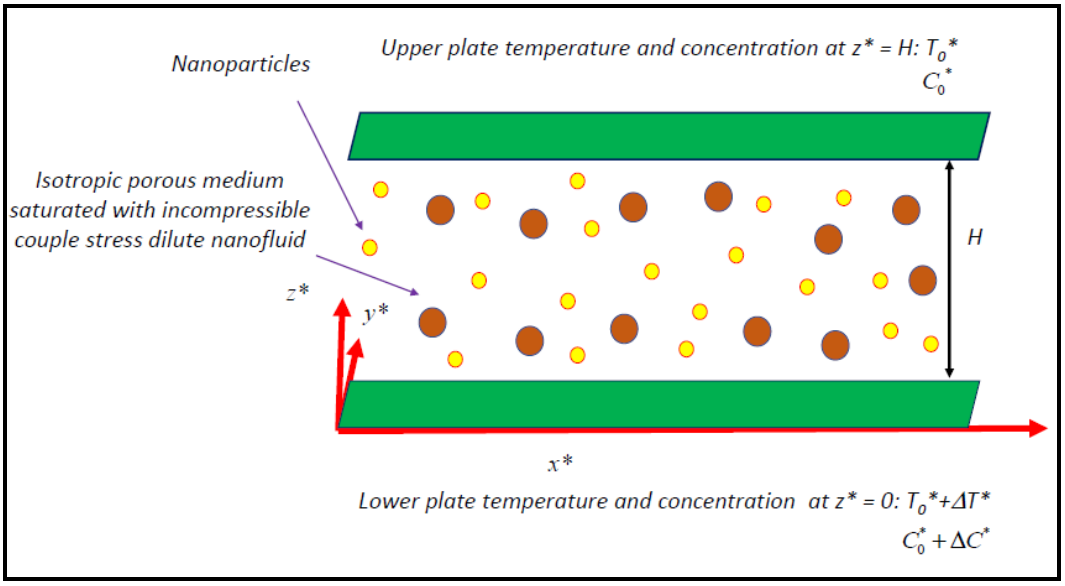

Fig. 1 Physical model

The temperatures and concentrations at the lower and upper boundary are taken to be $T_0^* + \Delta T^*$, $C_0^* + \Delta C^*$, T_0^* and C_0^* respectively. The Oberbeck Boussinesq approximation is employed. In the linear stability theory being applied here, the temperature change in the fluid is assumed to be small in comparison with T_0^*. The mass conservation equation takes the form:

$$\nabla^*.\mathbf{v}_D^* = 0 \tag{1}$$

Here, $\mathbf{v}_D^*$ is the nanofluid Darcy velocity. We write $\mathbf{v}_D^* = \left(u^*, v^*, w^*\right)$.

In the presence of thermophoresis, the conservation equation for the nanoparticles, in the absence of chemical reactions, takes the form:

$$\frac{\partial \phi^*}{\partial t^*} + \frac{1}{\varepsilon}\mathbf{v}_D^*.\nabla\phi^* = \nabla^*.\left[D_B\nabla^*\phi^* + D_T\frac{\nabla^* T^*}{T^*}\right] \tag{2}$$

where ϕ^* is the nanoparticle volume fraction, ε is the porosity, T^* is the temperature, D_B is the Brownian diffusion coefficient, and D_T is the thermophoretic diffusion coefficient. Introducing a buoyancy force, adopting the Boussinesq approximation, and using the Darcy model for a porous medium, the momentum equation can be written as:

$$\frac{\rho}{\varepsilon}\frac{\partial \mathbf{v}_D^*}{\partial t^*} = -\nabla^* p^* - \frac{1}{K}\left(\mu_{eff} - \mu_C\right)\mathbf{v}_{\mathrm{D}}^* + \rho\,\mathrm{g} \tag{3}$$

Here ρ is the overall density of the nanofluid, which we now assume to be given by:

$$\rho = \phi^*\rho_{\mathrm{p}} + \left(1-\phi^*\right)\rho_0\left[1-\beta_{\mathrm{T}}\left(T^* - T_0^*\right) - \beta_C\left(C^* - C_0^*\right)\right] \tag{4}$$

where C is the concentration, ρ_{p} is the particle density, ρ_0 is a reference density for the fluid, β_{T} is the thermal volumetric expansion coefficient and β_C is the analogous solutal coefficient. The thermal energy (heat conservation) equation for the nanofluid can be written as:

$$\begin{aligned}\left(\rho c\right)_{\mathrm{m}}\frac{\partial T^*}{\partial t^*} + \left(\rho c\right)_{\mathrm{f}}\mathbf{v}_{\mathrm{D}}^*.\nabla^* T^* &= k_{\mathrm{m}}\nabla^{*2}T^* + \varepsilon\left(\rho c\right)_{\mathrm{p}}\left[D_{\mathrm{B}}\nabla^*\phi^*.\nabla T^* + D_{\mathrm{T}}\frac{\nabla T^*.\nabla T^*}{T_0^*}\right] \\ &\quad + \rho c\, D_{TC}\nabla^{*2}C^*\end{aligned} \tag{5}$$

Here c is the fluid specific heat (at constant pressure), k_m is the overall thermal conductivity of the porous medium saturated by the nanofluid, c_p is the nanoparticle specific heat of the material constituting the nanoparticles, D_{TC} is a diffusivity of Dufour type.

To this we add a conservation equation for the solute (distinct species from the nanoparticles) of the form:

$$\frac{\partial C^*}{\partial t^*} + \frac{1}{\varepsilon}\mathbf{v}_{\mathrm{D}}^*.\nabla^* C^* = D_{Sm}\nabla^{*2}C^* + D_{CT}\nabla^{*2}T^* \tag{6}$$

Here D_{Sm} is the solutal diffusivity for the porous medium and D_{CT} is a diffusivity of Soret type. It has been assumed that the nanoparticles do not affect the transport of the solute.

Thus,

$$k_m = \varepsilon k_{eff} + (1-\varepsilon)k_s \tag{7}$$

where ε is the medium porosity, k_{eff} is the effective conductivity of the nanofluid (fluid plus nanoparticles), and k_s is the conductivity of the solid material forming the matrix of the porous medium.

We now introduce the viscosity and thermal conductivity dependence on nanoparticle fraction. Following Tiwari and Das [33], we adopt the following formulae based on mixture theory:

$$\frac{\mu_{eff}}{\mu_f} = \frac{1}{(1-\phi^*)^{2.5}} \tag{8}$$

$$\frac{k_{eff}}{k_f} = \frac{(k_p + 2k_f) - 2\phi^*(k_f - k_p)}{(k_p + 2k_f) + \phi^*(k_f - k_p)} \tag{9}$$

Here k_f and k_p are the thermal conductivities of the fluid and the nanoparticles, respectively. Equation (8) was obtained by Brinkman [34], and (9) is the Maxwell-Garnett formula for a suspension of spherical particles originally reported by Maxwell [35].

In the case where ϕ^* is small compared with unity, we can approximate these formulae by:

$$\frac{\mu_{eff}}{\mu_f} = 1 + 2.5\phi^*, \quad \frac{k_{eff}}{k_f} = \frac{(k_p + 2k_f) - 2\phi^*(k_f - k_p)}{(k_p + 2k_f) + \phi^*(k_f - k_p)} = 1 + 3\phi^* \frac{(k_p - k_f)}{(k_p + 2k_f)} \tag{10}$$

We assume that the temperature and the volumetric fraction of the nanoparticles are constant on the boundaries. The appropriate boundaries conditions are therefore:

$$w^* = 0,\ T^* = T_0^* + \Delta T^*, C^* = C_0^* + \Delta C^*,\ \phi^* = \phi_0^* \text{ at } z^* = 0, \tag{11a}$$

$$w^* = 0,\ T^* = T_0^*,\ C^* = C_0^*,\ \phi^* = \phi_1^* \text{ at } z^* = H \tag{11b}$$

We introduce dimensionless variables as follows. We define:

$$(x, y, z) = (x^*, y^*, z^*)/H,\ t = t^*\alpha_m/\sigma H^2,\ (u, v, w) = (u^*, v^*, w^*)H/\alpha_m, ,$$

$$p = p^*K/\mu_f\alpha_m,\ \phi = \frac{\phi^* - \phi_0^*}{\phi_1^* - \phi_0^*},\ T = \frac{T^* - T_0^*}{\Delta T^*},\ C = \frac{C^* - C_0^*}{\Delta C^*},\ C_P = \frac{\mu_C}{\mu_{eff} H^2} \tag{12}$$

where

$$\alpha_m = \frac{k_m}{(\rho c_p)_f}, \quad \sigma = \frac{(\rho c_p)_m}{(\rho c_p)_f}$$

We also define

$$\tilde{\mu} = \frac{\mu_{eff}}{\mu_f}, \quad k = \frac{k_p}{k_f}, \quad \tilde{k}_s = \frac{k_s}{k_f}, \quad \tilde{k} = \frac{k_m}{k_f} \tag{13}$$

From (7), (10) and (13) we have:

$$\tilde{\mu} = 1 + 2.5[\phi_0^* + \phi(\phi_1^* - \phi_0^*)], \; \tilde{k} = \varepsilon\left\{1 + 3[\phi_0^* + \phi(\phi_1^* - \phi_0^*)]\frac{\tilde{k}_p - 1}{\tilde{k}_p + 2}\right\} + (1-\varepsilon)\tilde{k}_s \tag{14}$$

Then Eqn. (1) and (3) with (4), (5), (2), (11) take the form:

$$\nabla.\mathbf{v} = 0 \tag{15}$$

$$\gamma_a \frac{\partial \mathbf{v}}{\partial t} = -\nabla p - \tilde{\mu}\,\mathbf{v}\left(1 - Cp\nabla^2\right) - Rm\hat{e}_z + Ra_T T\hat{e}_z + \left(Rs/Le\right)C\hat{e}_z - Rn\,\phi\,\hat{e}_z \tag{16}$$

$$\frac{\partial T}{\partial t} + \mathbf{v}.\nabla T = \tilde{k}\nabla^2 T + \frac{N_B}{Ln}\nabla\phi.\nabla T + \frac{N_A N_B}{Ln}\nabla T.\nabla T + N_{TC}\nabla^2 C \tag{17}$$

$$\frac{1}{\sigma}\frac{\partial C}{\partial t} + \frac{1}{\varepsilon}\mathbf{v}.\nabla C = \frac{1}{Le}\nabla^2 C + N_{CT}\nabla^2 T \tag{18}$$

$$\frac{1}{\sigma}\frac{\partial \phi}{\partial t} + \frac{1}{\varepsilon}\mathbf{v}.\nabla\phi = \frac{1}{Ln}\nabla^2\phi + \frac{N_A}{Ln}\nabla^2 T \tag{19}$$

$$w = 0,\; T = 1,\; C = 1,\; \phi = 0 \;\; at \;\; z = 0, \quad w = 0,\; T = 0,\; C = 0,\; \phi = 0 \;\; at \;\; z = 1 \tag{20}$$

Here

$$\gamma_a = \frac{\varepsilon}{\sigma Va}, Ln = \frac{\alpha_m}{D_B}, Va = \frac{\varepsilon^2 \,\mathrm{Pr}}{Da}, Ra_T = \frac{\rho g \beta_T K H \Delta T^*}{\mu_f \alpha_m}, \mathrm{Pr} = \frac{\mu_f}{\rho\,\alpha_m}, Da = \frac{K}{H^2},$$

$$Rs = \frac{\rho g \beta_C K H \Delta C^*}{\mu_f\, D_{Sm}}, Rm = \frac{\left[\rho_p \phi_0^* + \rho(1-\phi_0^*)\right] gKH}{\mu_f \alpha_m}, Rn = \frac{(\rho_p - \rho)(\phi_1^* - \phi_0^*) gKH}{\mu_f \alpha_m},$$

$$N_A = \frac{D_T \Delta T^*}{D_B T_c^* (\phi_1^* - \phi_0^*)}, \qquad N_B = \frac{\varepsilon(\rho c)_p (\phi_1^* - \phi_0^*)}{(\rho c)_f}, \qquad Le = \frac{\alpha_f}{D_S}, \qquad N_{TC} = \frac{D_{TC}\Delta C^*}{\alpha_m \Delta T^*},$$

$$N_{CT} = \frac{D_{CT}\,\Delta T^*}{\alpha_m \Delta C^*}$$

The parameter γ_a is the non dimensional acceleration coefficient, Ln is a thermo-nanofluid Lewis number, Va is a Vadász number, Ra_T is the familiar thermal Rayleigh–Darcy number, Pr is the Prandtl number, *Da* is the Darcy number, *Rs* is the familiar solutal Rayleigh number, The new parameters *Rm* and *Rn* may be regarded as a basic-density Rayleigh number and a concentration Rayleigh number, respectively. The parameter N_A is a modified diffusivity ratio and similar to the Soret parameter arising in cross-diffusion phenomena in solutions, while N_B is a modified particle-density increment, *Le* is the familiar thermo-solutal Lewis number.

In the spirit of the Oberbeck–Boussinesq approximation, (16) has been linearized by the neglect of a term proportional to the product of ϕ and *T*. This assumption is likely to be valid in the case of small temperature gradients in a dilute suspension of nanoparticles.

3. Solutions

3.1 Basic solution

We seek a time-independent quiescent solution of Eqns. (15) - (20) with temperature and nanoparticle volume fraction varying in the *z*-direction only, that is a solution of the form

$$\mathbf{v}=0,\ p=p_b(z),\ T=T_b(z),\ C=C_b(z),\ \phi=\phi_b(z) \tag{21}$$

Equations (16)-(19) reduce to:

$$0=-\frac{dp_b}{dz}-Rm+Ra_T\,T_b+\left(Rs/Le\right)C_b-Rn\,\phi_b \tag{22}$$

$$\tilde{k}\frac{d^2T_b}{dz^2}+\frac{N_B}{Ln}\frac{d\phi_b}{dz}+\frac{N_AN_B}{Ln}\left(\frac{dT_b}{dz}\right)^2+N_{TC}\frac{d^2C_b}{dz^2}=0 \tag{23}$$

$$\frac{1}{Le}\frac{d^2C_b}{dz^2}+N_{CT}\frac{d^2T_b}{dz^2}=0 \tag{24}$$

$$\frac{d^2\phi_b}{dz^2}+N_A\frac{d^2T_b}{dz^2}=0 \tag{25}$$

According to Buongiorno [10], for most practical nanofluids, $Ln/\left(\phi_1^*-\phi_0^*\right)$ is large, of order 10^5–10^6, and since the nanoparticle fraction decrement is typically no smaller

than 10^3 this means so that *Ln* is large, of order 10^2–10^3, while N_A is no greater than about 10. Using this approximation, the basic solution is found to be:

$$T_b = 1 - z\,,\ C_b = 1 - z \text{ and so } \phi_b = z \tag{26}$$

3.2 Perturbation solution

We now superimpose perturbations on the basic solution as follows:

$$\mathbf{v} = \mathbf{v}'\ ,\ p = p_b + p'\,,\ T = T_b + T'\,, C = C_b + C'\,,\ \phi = \phi_b + \phi' \tag{27}$$

These are substituted in Eqns. (13)–(19), and after linearizing by neglecting products of primed quantities, the following equations are obtained when Eqn. (26) is used:

$$\nabla.\mathbf{v}' = 0 \tag{28}$$

$$\gamma_a \frac{\partial \mathbf{v}'}{\partial t} = -\nabla p' - \tilde{\mu}\left(1 - Cp\nabla^2\right)\mathbf{v}' + Ra_T T'\hat{e}_z + \left(Rs/Le\right)C'\hat{e}_z - Rn\phi'\hat{e}_z \tag{29}$$

$$\frac{\partial T'}{\partial t} - w' = \tilde{k}\nabla^2 T' + \frac{N_B}{Ln}\left(\frac{\partial T'}{\partial z} - \frac{\partial \phi'}{\partial z}\right) - \frac{2N_A N_B}{Ln}\frac{\partial T'}{\partial z} + N_{TC}\nabla^2 C' \tag{30}$$

$$\frac{1}{\sigma}\frac{\partial C'}{\partial t} + \frac{1}{\varepsilon}w' = \frac{1}{Le}\nabla^2 C + N_{CT}\nabla^2 T \tag{31}$$

$$\frac{1}{\sigma}\frac{\partial \phi'}{\partial t} + \frac{1}{\varepsilon}w' = \frac{1}{Ln}\nabla^2 \phi' + \frac{N_A}{Ln}\nabla^2 T' \tag{32}$$

$$w' = 0\,, T' = 0\,, C' = 0,\ \phi' = 0 \text{ at } z = 0 \text{ and at } z = 1 \tag{33}$$

Next the viscosity and conductivity distributions can be approximated by substituting the basic solution expression for ϕ, namely that given by (26), into (14), we obtain:

$$\tilde{\mu}(z) = 1 + 2.5\left[\phi_0^* + \phi(\phi_1^* - \phi_0^*)\,z\right],\ \tilde{k}(z) = \varepsilon\left\{1 + 3\left[\phi_0^* + \phi\left(\phi_1^* - \phi_0^*\right)z\right]\frac{\tilde{k}_p - 1}{\tilde{k}_p + 2}\right\} + (1-\varepsilon)\tilde{k}_s \tag{34}$$

It will be noted that the parameter *Rm* is essentially a measure of the basic static pressure gradient and is not involved in these and subsequent equations. The emerging problem has properties are heterogeneous. These are now the viscosity and thermal conductivity (rather that the more conventional permeability and thermal conductivity) and

the methodology of many studies is employed, as surveyed by Nield [36]. We assume that the heterogeneity is weak in the sense that the maximum variation of a property over the domain considered is small compared with the mean value of that property in the same domain. The seven unknowns $\mathrm{u}', \mathrm{v}', \mathrm{w}', \mathrm{p}', \mathrm{T}', C', \phi'$ can be reduced to four by operating on Eqn. (29) with $\hat{e}_z$ curl curl and using the identity curl curl $\equiv$ grad div - ∇^2 together with (28) and the weak heterogeneity approximation. The result is:

$$\left(\left(\tilde{\mu}(z)+s\gamma_a\right)-\tilde{\mu}(z)Cp\nabla^2\right)\nabla^2 w' = Ra_T\nabla_H^2 T' + \left(Rs/Le\right)\nabla_H^2 C' - Rn\nabla_H^2\phi' \tag{35}$$

Here ∇_H^2 is the two-dimensional Laplacian operator on the horizontal plane.

The differential equations (35), (29), (30), (31), (32) and the boundary conditions (33) constitute a *linear* boundary-value problem which can be solved using the method of normal modes. We write:

$$\left(w', T', C', \phi'\right) = \left[W(z), \Theta(z), \Sigma(z), \Phi(z)\right]\exp\left(st + ilx + imy\right) \tag{36}$$

Substituting into the differential equations leads to:

$$\left(\left(\tilde{\mu}(z)+s\gamma_a\right)-\tilde{\mu}(z)C_P\left(D^2-\alpha^2\right)\right)\left(D^2-\alpha^2\right)W + Ra_T\,\alpha^2\,\Theta + \left(Rs/Le\right)\alpha^2\,\Sigma - Rn\,\alpha^2\,\Phi = 0 \tag{37}$$

$$W + \left(\left(D^2-\alpha^2\right)\tilde{k}(z) + \frac{N_B}{Ln}D - \frac{2N_AN_B}{Ln}D - s\right)\Theta - \frac{N_B}{Ln}D\Phi + N_{TC}\left(D^2-\alpha^2\right)\Sigma = 0 \tag{38}$$

$$\frac{1}{\varepsilon}W + \frac{1}{Le}\left(D^2-\alpha^2-\frac{1}{\sigma}s\right)\Sigma + N_{CT}\left(D^2-\alpha^2\right)\Theta = 0 \tag{39}$$

$$\frac{1}{\varepsilon}W - \frac{N_A}{Ln}\left(D^2-\alpha^2\right)\Theta - \left(\frac{1}{Ln}\left(D^2-\alpha^2\right)-\frac{1}{\sigma}s\right)\Phi = 0 \tag{40}$$

$$W = 0,\ \Theta = 0, \Sigma = 0,\ \Phi = 0 \quad \text{at } z = 0 \text{ and } z = 1 \tag{41}$$

where s is the perturbation growth rate which is in general of complex form, and the following notation, is then used:

$$D \equiv \frac{d}{dz} \text{ and } \alpha = (l^2+m^2)^{1/2}\ . \tag{42}$$

Thus α is a dimensionless horizontal wave number.

For neutral stability the real part of s is zero. Hence we now write $s = i\omega$, where ω is real and is a dimensionless frequency.

We now employ a Galerkin-type weighted residuals method to obtain an approximate solution to the system of (37)–(41). We choose the following trial functions (satisfying the boundary conditions), $W_p, \Theta_p, \Sigma_p, \Phi_p ; p = 1, 2, 3.....$ and write:

$$\mathrm{W} = \sum_{p=1}^{N} A_p W_p , \Theta = \sum_{p=1}^{N} B_p \Theta_P , \Sigma = \sum_{p=1}^{N} C_p \Sigma_p , \Phi = \sum_{p=1}^{N} D_p \Phi_P \tag{43}$$

Insertion into Eqns. (37)–(41), and making the expressions on the left-hand sides of those equations (the residuals) orthogonal to the trial functions, generates a system of 4*N* linear algebraic equations in the 4*N* unknowns $A_p, B_p, C_p,$ D_p, p =1, 2, . . . *N*. The vanishing of the determinant of coefficients produces the eigenvalue equation for the system. One can regard Ra_T as the eigenvalue. Thus Ra_T is found in terms of the other parameters.

Trial functions satisfying the boundary condition (41) can be chosen as:

$$W_p = \Theta_p = \Phi_p = \Sigma_p = \sin p\pi z \; ; \; p = 1, 2, 3, \ldots \tag{44}$$

The eigenvalue equation is

$$\det M = 0 \tag{45}$$

where,

$$M = \begin{bmatrix} M_{11} & M_{12} & M_{13} & M_{14} \\ M_{21} & M_{22} & M_{23} & M_{24} \\ M_{31} & M_{32} & M_{33} & M_{34} \\ M_{41} & M_{42} & M_{43} & M_{44} \end{bmatrix} \tag{46}$$

and, for $i, j = 1, 2, \ldots, N$.

$$\left(M_{11}\right)_{ij} = -\left\langle\left(\tilde{\mu}(z)+\gamma_a s-\tilde{\mu}(z)C_P D^2\right)W_j D^2 W_i\right\rangle+\alpha^2\left\langle\left(\tilde{\mu}(z)+\gamma_a s-\tilde{\mu}(z)C_P D^2\right)W_j W_i\right\rangle$$

$$\left(M_{12}\right)_{ij} = -Ra_T\alpha^2\left\langle W_j\Theta_i\right\rangle$$

$$\left(M_{13}\right)_{ij} = -\left(Rs/Le\right)\alpha^2\left\langle W_j\Sigma_i\right\rangle$$

$$\left(M_{14}\right)_{ij} = Rn\alpha^2\left\langle W_j\Phi_i\right\rangle$$

$$\left(M_{21}\right)_{ij} = -\left\langle\Theta_j W_i\right\rangle$$

$$\left(M_{22}\right)_{ij} = -\left\langle\tilde{k}(z)\Theta_j D^2\Theta_i\right\rangle+\alpha^2\left\langle\tilde{k}(z)\Theta_j\Theta_i\right\rangle+s\left\langle\Theta_j\Theta_i\right\rangle+\left(\frac{2N_A N_B}{Ln}-\frac{N_B}{Ln}\right)\left\langle\Theta_j D\Theta_i\right\rangle$$

$$\left(M_{23}\right)_{ij} = -\left\langle N_{TC}\Theta_j D^2\Sigma_i\right\rangle+\alpha^2\left\langle N_{TC}\Theta_j\Sigma_i\right\rangle$$

$$\left(M_{24}\right)_{ij} = \frac{N_B}{Ln}\left\langle\Theta_j D\Phi_i\right\rangle$$

$$\left(M_{31}\right)_{ij} = -\frac{1}{\varepsilon}\left\langle\Sigma_j W_i\right\rangle$$

$$\left(M_{32}\right)_{ij} = -\left\langle N_{CT}\Theta_i D^2\Sigma_j\right\rangle+\alpha^2\left\langle N_{CT}\Theta_i\Sigma_j\right\rangle$$

$$\left(M_{33}\right)_{ij} = \frac{1}{Le}\left(-\left\langle\Sigma_j D^2\Sigma_i\right\rangle+\alpha^2\left\langle\Sigma_j\Sigma_i\right\rangle+\frac{s}{\sigma}\left\langle\Sigma_j\Sigma_i\right\rangle\right)$$

$$\left(M_{34}\right)_{ij} = 0$$

$$\left(M_{41}\right)_{ij} = -\frac{1}{\varepsilon}\left\langle\Phi_j W_i\right\rangle$$

$$\left(M_{42}\right)_{ij} = \frac{N_A}{Ln}\left(\left\langle\Phi_j D^2\Theta_i\right\rangle-\alpha^2\left\langle\Phi_j\Theta_i\right\rangle\right)$$

$$\left(M_{43}\right)_{ij} = 0$$

$$\left(M_{44}\right)_{ij} = \frac{1}{Ln}\left(\left\langle\Phi_j D^2\Phi_i\right\rangle-\alpha^2\left\langle\Phi_j\Phi_i\right\rangle\right)-\frac{s}{\sigma}\left\langle\Phi_j\Phi_i\right\rangle \qquad (47)$$

Here $\left\langle f(z)\right\rangle \equiv \int_0^1 f(z)\,dz$. In the present case, where viscosity and thermal conductivity variations are incorporated, the critical wave number is unchanged, and the stability boundary becomes:

$$Ra_T = \frac{1}{\alpha^2}\left(\frac{JN_{TC}}{\varepsilon}\left(\frac{J}{Ln}+\frac{s}{\sigma}\right)-\frac{1}{Le}\left(J+\frac{s}{\sigma}\right)\left(\frac{J}{Ln}+\frac{s}{\sigma}\right)\right)^{-1}$$
$$\left[\begin{array}{l}\left((-J)\left(\frac{J\eta+s}{Le}\right)\left(\frac{J}{Ln}+\frac{s}{\sigma}\right)\left(J+\frac{s}{\sigma}\right)+J^3N_{TC}N_{CT}\left(\frac{J}{Ln}+\frac{s}{\sigma}\right)\right)(\nu+s\gamma_a)+\\ \nu C_P\left(J^4N_{TC}N_{CT}\left(\frac{J}{Ln}+\frac{s}{\sigma}\right)-J^2\left(\frac{J\eta+s}{Le}\right)\left(\frac{J}{Ln}+\frac{s}{\sigma}\right)\left(J+\frac{s}{\sigma}\right)\right)+\\ \frac{Rs\alpha^2}{Le}\left(-JN_{CT}\left(\frac{J}{Ln}+\frac{s}{\sigma}\right)+\left(\frac{J\eta+s}{\varepsilon}\right)\left(\frac{J}{Ln}+\frac{s}{\sigma}\right)\right)+\\ Rn\alpha^2\left(\frac{N_AJ}{LeLn}\left(J+\frac{s}{\sigma}\right)+\left(\frac{J\eta+s}{Le\varepsilon}\right)\left(J+\frac{s}{\sigma}\right)-JN_{TC}\left(\frac{N_AJ}{\varepsilon Ln}+\frac{JN_{CT}}{\varepsilon}\right)\right)\end{array}\right] \quad (48)$$

where

$$J = (\pi^2+\alpha^2),\ \nu = 1+1.25\left(\phi_1^*+\phi_0^*\right)$$

$$\eta = \varepsilon+(1-\varepsilon)\tilde{k}_s+\frac{3\left(\phi_1^*+\phi_0^*\right)\varepsilon}{2}\left(\frac{\tilde{k}_p-1}{\tilde{k}_p+2}\right) \quad (49)$$

We observe that when there is no thermal conductivity variation (that is $\eta = 1$, as when $\tilde{k}_s = 1$ and $\tilde{k}_p = 1$) the effect of viscosity variation is to *increase* the critical Rayleigh number by a factor ν. The additional effect of thermal conductivity variation η is expressed by Eqn. (49). When $\tilde{k}_s = 1$, the maximum value of η is $2.5\left(\phi_1^*+\phi_0^*\right)$ which is achieved when $\varepsilon = 1$ and $\tilde{k}_p \to \infty$.

It is worth noting that the factor ν comes from the mean value of $\tilde{\mu}(z)$ over the range [0,1] and the factor η is the mean value of $\tilde{k}(z)$ over the same range. This implies that when evaluating the critical Rayleigh number it is a good approximation to base that number on the mean values of the viscosity and thermal conductivity which are founded in turn on the basic solution for the *nanofluid fraction*.

3.3 Linear stability Analysis

3.3.1 Stationary Mode

By virtue of the principle of exchange of stabilities (i.e., steady case), we have s = 0 $\left(i.e., s = s_r + is_i = s_r = s_i = 0\right)$ at the margin of stability. For a first approximation we take $N = 1$. Then the Rayleigh number at which the *marginally stable steady mode* exists becomes:

$$Ra_T^{St} = \frac{1}{\alpha^2}\left(\frac{JN_{TC}}{\varepsilon}\left(\frac{J}{Ln}\right) - \frac{1}{Le}(J)\left(\frac{J}{Ln}\right)\right)^{-1}$$
$$\left[\begin{array}{l} \left((-J)\left(\frac{J\eta}{Le}\right)\left(\frac{J}{Ln}\right)(J) + J^3 N_{TC} N_{CT}\left(\frac{J}{Ln}\right)\right)\nu + \\ \nu C_P\left(J^4 N_{TC} N_{CT}\left(\frac{J}{Ln}\right) - J^3\left(\frac{J\eta}{Le}\right)\left(\frac{J}{Ln}\right)\right) \\ \frac{Rs\alpha^2}{Le}\left(-JN_{CT}\left(\frac{J}{Ln}\right) + \left(\frac{J\eta}{\varepsilon}\right)\left(\frac{J}{Ln}\right)\right) + \\ Rn\alpha^2\left(\frac{N_A J}{Le\,Ln}(J) + \left(\frac{J\eta}{Le\,\varepsilon}\right)(J) - JN_{TC}\left(\frac{N_A J}{\varepsilon\,Ln} + \frac{JN_{CT}}{\varepsilon}\right)\right) \end{array}\right] \tag{50}$$

In the case of double diffusion in a regular fluid, when N_{TC}, N_{CT} and N_A are all zero, Eqn. (50) reduces to $Ra_T^{St} + Rs = R_0$, where ($R_0 = 4\pi^2 = 39.48$ with $\alpha_c = \pi = 3.14$) as expected.

3.3.2 Oscillatory Mode

We now set $s = i\omega$, where $\omega = \mathrm{Im}(\omega)\left(Rp(\omega) = 0\right)$ in (48) and clear the complex quantities from the denominator, to obtain:

$$Ra_T = \Delta_1 + i\,\omega\,\Delta_2 \tag{51}$$

For oscillatory onset $\Delta_2 = 0$ $\left(\mathrm{Im}(\omega) \neq 0\right)$ and this gives a dispersion relation of the form (on dropping the subscript *i*)

$$b_1\left(\omega^2\right)^2 + b_2\left(\omega^2\right) + b_3 = 0 \tag{52}$$

Now Eq. (48) with $\Delta_2 = 0$ gives:

$$Ra_T^{Osc} = a_0\left(a_1 + \omega^2 a_2\right) \tag{53}$$

where $b_1, b_2,$ and b_3 and $a_0, a_1,$ and a_2 and Δ_1 and Δ_2 are not presented here for brevity.

We find the *oscillatory neutral solutions* from Eqn. (53). This involves determining the number of positive solutions of Eqn. (52). If there are none, then no oscillatory instability is possible. If there are two, then the minimum (over a^2) of Eqn (53) with ω^2 given by Eqn. (52) gives the oscillatory neutral Rayleigh number. Since Eqn. (52) is quadratic in ω^2, it can give rise to more than one positive value of ω^2 for fixed values of the parameters *Rn*, *Ln*, N_A, σ, γ_a, ν, η, and λ. However, the numerical solution of (52) for the range of parameters considered here gives only one positive value of ω^2 indicating that there exists *only one oscillatory neutral solution*. The analytical expression for oscillatory Rayleigh number given by Eqn. (53) is minimized with respect to the wavenumber numerically, after substituting for ω^2 (> 0) from Eqn. (52), for various values of physical parameters in order to establish their effects on the onset of oscillatory convection.

3.3.3 Nonlinear stability analysis

For simplicity, we consider the case of two-dimensional convective rolls, assuming all physical quantities to be independent of *y*. Eliminating the pressure and introducing the stream function we obtain:

$$\left(\nu + s\,\gamma_a\right)\nabla^2\Psi + \nu C_P \nabla^4\Psi + Ra_T \frac{\partial T}{\partial x} + \left(\frac{Rs}{Le}\right)\frac{\partial C}{\partial x} - Rn\frac{\partial S}{\partial x} = 0 \tag{54}$$

$$\frac{\partial T}{\partial t} + \frac{\partial \Psi}{\partial x} = \eta\nabla^2 T + \frac{\partial\left(\Psi, T\right)}{\partial\left(x, z\right)} + N_{TC}\nabla^2 C \tag{55}$$

$$\frac{1}{\sigma}\frac{\partial S}{\partial T} + \frac{1}{\varepsilon}\frac{\partial \Psi}{\partial x} = \frac{1}{Ln}\nabla^2 S + \frac{N_A}{Ln}\nabla^2 T + \frac{1}{\varepsilon}\frac{\partial(\Psi, S)}{\partial(x, z)} \tag{56}$$

$$\frac{1}{\sigma}\frac{\partial C}{\partial T} + \frac{1}{\varepsilon}\frac{\partial \Psi}{\partial x} = \frac{1}{Le}\nabla^2 C + N_{CT}\nabla^2 T + \frac{1}{\varepsilon}\frac{\partial(\Psi, C)}{\partial(x, z)} \tag{57}$$

We solve Eqns. (54)–(57) subjecting them to *stress-free*, isothermal, iso-nano-concentration boundary conditions:

$$\psi = \frac{\partial^2\psi}{\partial z^2} = T = S = C = 0 \text{ at } z = 0, 1 \tag{58}$$

To perform a *local non-linear stability analysis,* we take the following Fourier expressions:

$$\psi = \sum_{n=1}^{\infty}\sum_{m=1}^{\infty} A_{mn}\left(t\right) sin\left(m\alpha x\right) sin\left(n\pi z\right)$$

$$T = \sum_{n=1}^{\infty}\sum_{m=1}^{\infty} B_{mn}(t)\cos\left(m\alpha x\right)sin\left(n\pi z\right)$$

$$S = \sum_{n=1}^{\infty}\sum_{m=1}^{\infty} C_{mn}(t)\cos\left(m\alpha x\right)sin\left(n\pi z\right)$$

$$C = \sum_{n=1}^{\infty}\sum_{m=1}^{\infty} D_{mn}(t)\cos\left(m\alpha x\right)sin\left(n\pi z\right) \tag{59}$$

Further, we take the modes (1, 1) for stream function, and (0, 2) and (1, 1) for temperature, and nanoparticle concentration, to get:

$$\psi = A_{11}(t)\,sin(\alpha x)\,sin(\pi z)$$

$$T = B_{11}(t)\cos(\alpha x)\,sin(\pi z) + B_{02}(t)\,sin(2\pi z)$$

$$S = C_{11}(t)\cos(\alpha x)\,sin(\pi z) + C_{02}(t)\,sin(2\pi z)$$

$$C = D_{11}(t)\cos(\alpha x)\,sin(\pi z) + D_{02}(t)\,sin(2\pi z) \tag{60}$$

where the amplitudes $A_{11}(t)$, $B_{11}(t)$, $B_{02}(t)$, $C_{11}(t)$, $C_{02}(t)$, $D_{11}(t)$ and $D_{02}(t)$ are functions of time and are to be determined from the dynamics of the system.

The first effect of non-linearity is to distort the temperature and concentration fields through the interaction of ψ, T and ψ, S and also ψ, C. The distortion of these fields will correspond to a change in the horizontal mean, i.e., a component of the form $sin(2\pi z)$ will be generated. It is obvious that ψ is minimally represented, since it is the simplest possible form for satisfying the boundary condition; it is also the form of ψ for the stability problem. The amplitude $A_{11}(t)$ is (generally) a function of time and must be determined. The term $B_{11}(t)\cos(\alpha x)\,sin(\pi z)$ is also a minimal representation for θ and is included as it must balance the stream function term in the heat transport equation. The term $B_{02}(t)\,sin(2\pi z)$ represents the minimal representation for the distortion of the mean temperature field. The reason for the value 2 in the argument is that the mean temperature field is distorted by the convective term $\psi\theta$, in the heat equation; since both ψ and θ have components proportional to $sin(\pi z)$, this will force a $sin(2\pi z)$ dependence on the mean temperature. Similar remarks apply to the solute concentration and nanoparticle concentrations.

Taking the orthogonality condition with the eigenfunctions associated with the considered minimal model, we get:

$$\frac{dA_{11}(t)}{dt}=\frac{1}{\gamma_a\delta^2}\left[\alpha Rn\,C_{11}(t)-\alpha Ra_T\,B_{11}(t)-\frac{\alpha Rs\,D_{11}(t)}{Le}-\nu\delta^2A_{11}(t)-\nu\,C_P\delta^4A_{11}(t)\right]$$

$$\frac{dB_{11}}{dt}=-\left[\alpha A_{11}(t)+\eta\,\delta^2B_{11}(t)+\alpha\,\pi\,A_{11}(t)\,B_{02}(t)+N_{TC}\,\delta^2D_{11}(t)\right]$$

$$\frac{dB_{02}}{dt}=-\eta\,4\pi^2B_{02}(t)+\frac{\alpha\pi}{2}A_{11}(t)B_{11}(t)-N_{TC}\,4\pi^2D_{02}(t)$$

$$\frac{dC_{11}}{dt}=-\sigma\left[\frac{1}{\varepsilon}\alpha A_{11}(t)+\delta^2\left(\frac{C_{11}(t)}{Ln}+\frac{N_A}{Ln}B_{11}(t)\right)+\frac{1}{\varepsilon}\alpha\pi A_{11}(t)C_{02}(t)\right]$$

$$\frac{dC_{02}}{dt}=-\sigma\left[\frac{1}{Ln}4\pi^2C_{02}(t)+4\pi^2B_{02}(t)\frac{N_A}{Ln}-\frac{a\pi}{2\varepsilon}A_{11}(t)C_{11}(t)\right]$$

$$\frac{dD_{11}}{dt}=-\sigma\left[\frac{1}{\varepsilon}\alpha A_{11}(t)+\delta^2\left(\frac{D_{11}(t)}{Le}+N_{CT}B_{11}(t)\right)+\frac{1}{\varepsilon}\alpha\pi A_{11}(t)D_{02}(t)\right]$$

$$\frac{dD_{02}}{dt}=-\sigma\left[\frac{1}{Le}4\pi^2D_{02}(t)+4\pi^2B_{02}(t)N_{CT}-\frac{a\pi}{2\varepsilon}A_{11}(t)D_{11}(t)\right] \qquad (61)$$

In the case of steady motion $\frac{d(\ )}{dt}=D_i=0$, (i = 1, 2, .., 7) and writing all D_i's in terms of A_{11} leads to:

$$D_1=\frac{1}{\gamma_a\delta^2}\left[\alpha Rn\,C_{11}(t)-\alpha Ra_T\,B_{11}(t)-\frac{\alpha Rs\,D_{11}(t)}{Le}-\nu\delta^2A_{11}(t)\right]$$

$$D_2=-\left[\alpha A_{11}(t)+\eta\,\delta^2B_{11}(t)+\alpha\,\pi\,A_{11}(t)\,B_{02}(t)+N_{TC}\,\delta^2D_{11}(t)\right]$$

$$D_3=-\eta\,4\pi^2B_{02}(t)+\frac{\alpha\pi}{2}A_{11}(t)B_{11}(t)-N_{TC}\,4\pi^2D_{02}(t)$$

$$D_4=-\sigma\left[\frac{1}{\varepsilon}\alpha A_{11}(t)+\delta^2\left(\frac{C_{11}(t)}{Ln}+\frac{N_A}{Ln}B_{11}(t)\right)+\frac{1}{\varepsilon}\alpha\pi A_{11}(t)C_{02}(t)\right]$$

$$D_5=-\sigma\left[\frac{1}{Ln}4\pi^2C_{02}(t)+4\pi^2B_{02}(t)\frac{N_A}{Ln}-\frac{a\pi}{2\varepsilon}A_{11}(t)C_{11}(t)\right]$$

$$D_6=-\sigma\left[\frac{1}{\varepsilon}\alpha A_{11}(t)+\delta^2\left(\frac{D_{11}(t)}{Le}+N_{CT}B_{11}(t)\right)+\frac{1}{\varepsilon}\alpha\pi A_{11}(t)D_{02}(t)\right]$$

$$D_7 = --\sigma\left[\frac{1}{Le}4\pi^2 D_{02}(t) + 4\pi^2 B_{02}(t)N_{CT} - \frac{a\pi}{2\varepsilon}A_{11}(t)D_{11}(t)\right]$$

and $D_1 = D_2 = D_3 = D_4 = D_5 = D_6 = D_7 = 0$ (62)

The above system of simultaneous autonomous ordinary differential equations is solved numerically using a Runge–Kutta–Gill method. One may also conclude that the trajectories of the above equations will be confined to the finiteness of the ellipsoid. Thus, the effect of the parameters *Rn*, *Ln*, N_A on the trajectories is to attract them to a set of measure zero, or to a fixed point to say.

3.3.4 Heat and Nanoparticle Concentration Transport

The Thermal Nusselt number *NuT* is defined as

$$NuT = \frac{\text{Heat transport by (conduction + convection)}}{\text{Heat transport by conduction}} = 1 + \left[\frac{\int_0^{2\pi}\frac{\partial T}{\partial z}\,dx}{\int_0^{2\pi/a}\frac{\partial T_B}{\partial z}\,dx}\right]_{z=0} \quad (63)$$

Substituting expressions (26) and (60) in the above equation we get:

$$NuT = 1 - 2\pi B_{02}(t)$$

The nanoparticle concentration Nusselt number *NuF* is defined similar to the thermal Nusselt number. Following the procedure adopted for arriving at *NuT*, one can obtain the expression for *NuF* in the form:

$$NuF = \left(1 - 2\pi C_{02}(t)\right) + N_A\left(1 - 2\pi B_{02}(t)\right) \quad (64)$$

The solute concentration Nusselt number *NuC* is defined similar to the thermal Nusselt number. Following the procedure adopted for arriving at *NuT*, one can obtain the expression for *NuC* in the form:

$$NuC = \left(1 - 2\pi D_{02}(t)\right) + N_{CT}\left(1 - 2\pi B_{02}(t)\right) \quad (65)$$

4 . Results and discussion

The expressions of thermal Rayleigh number for stationary and oscillatory convections are given by Eqns. (50) and (53) respectively. Figure 2a-f shows the effect of various parameters on the neutral stability curves for stationary convection with variation in one of these parameters. The effect of Soret parameter N_{CT} and Dufour parameter N_{TC} on the thermal Rayleigh number is shown in Figs. 2a,b, respectively, from which it can be seen that as N_{CT} and N_{TC} increases Ra_T increases and hence N_{CT} and N_{TC} have a stabilizing effect on the system. From Fig. 2c, one can observe that as solutal Rayleigh number *Rs* increases, thermal Rayleigh number decreases which indicates that the solutal Rayleigh number *Rs advances* the onset of convection. The effects of viscosity ratio ν and thermal conductivity ratio η on the thermal Rayleigh number are depicted in Figs. 2 d,e respectively, which show that as ν and η increase, Ra_T increases which indicates that ν and η will stabilize the system. The effect of Soret parameter N_{CT}, Dufour parameter N_{TC} and solutal Rayleigh number *Rs* on thermal Rayleigh number Ra_T for stationary convection show similar results to those computed by Agarwal *et al.* [37]. Figure 2f reveals that as couple stress parameter C_P increases, Ra_T increases which indicates that C_P (stronger couple stress length effect) will stabilize the system.

Figures 3a-f displays the variation of thermal Rayleigh number for oscillatory convection with respect to various parameters. The effect of Soret parameter N_{CT} and Dufour parameter N_{TC} on the thermal Rayleigh number is shown in Figs. 3a, b, respectively, and evidently as N_{CT} and N_{TC} increase Ra_T increases and hence N_{CT} and N_{TC} have a stabilizing effect on the system. From Fig. 3c, one can observe that as solutal Rayleigh number *Rs* increases, thermal Rayleigh number decreases which means that the solutal Rayleigh number *Rs* advances the onset of convection. Figures 3d,e indicate that larger viscosity ratio ν and thermal conductivity ratio η both stabilize the system for oscillatory convection i.e. an increase in ν and η increases the thermal Rayleigh number thus delaying the onset of convection. From Fig. 3g one can observe that as couple stress parameter C_P increases, the thermal Rayleigh number also increases which effectively stabilizes the system. Thus, the couple stress parameter enhances the stability of the system for both stationary and oscillatory convection modes.

The nonlinear analysis provides not only the onset threshold of finite amplitude motion but also key information on heat and mass transfer at the boundaries (plates) in terms of thermal Nusselt number *NuT*, nanoparticle concentration Nusselt number *NuF* and solute concentration Nusselt number *NuC*. The Nusselt numbers are computed as functions of Ra_T, and the variations of these non-dimensional numbers with Ra_T for different parameter values are depicted in Figs. 4a-f, 5a-f and 6a-f respectively. In Figs. 4a-f, 5a-f and 6a-f it is observed that in each case, nanoparticle concentration Nusselt number *NuF* is always greater than both thermal Nusselt number *NuT* and solute concentration Nusselt number *NuC* and all Nusselt numbers start with the conduction state value 1 at the point of onset of steady finite amplitude convection. When Ra_T is increased beyond Ra_{Tc}, there is a sharp increase in the values of Nusselt numbers. However further increase in Ra_T will not change *Nu* and *Sh* significantly. It is to be noted that the upper bound of *NuT* is 3 (similar results were obtained by Malashetty *et al.* [38]). It should also be noted that the upper bound of *NuF* and *NuC* are not 3 (similar results were obtained by Bhadauria and Agarwal [39]). The upper bound of *NuT* remains 3 only for clear nanofluid. Whereas, the upper bound for *NuF* and *NuC* for clear fluid is 3 but for nanofluid it is not fixed.

From Figs. 4a and 5a we observe that as the Soret parameter N_{CT} increases, the value of *NuT* and *NuF* decrease, thus showing a decrease in the rate of heat and mass transfer at the plates, whereas the solute concentration Nusselt number *NuC* (Fig. 6a) increases with increase in Soret parameter N_{CT} implying that Soret parameter N_{CT} enhances the solute concentration Nusselt number. We observe that as the Dufour parameter N_{TC} (Figs. 4b, 5b and 6b) and solutal Rayleigh number *Rs* (Figs. 4c, 5c and 6c) increases, the value of *NuT*, *NuF* and *NuC* decreases, thus showing a decrease in the rate of heat and mass transport. As the viscosity ratio ν (Figs. 4d, 5d and 6d) and conductivity ratio η (Figs. 4e, 5e and 6e) increase all the Nusselt numbers increase, implying that ν and η enhance the heat and mass transport. From Figs. 4f, 5f, and 6f one can witness that as the couple stress parameter C_P increases, the values of *NuT, NuF* and *NuC* decrease, thus showing a decrease in the heat and mass transport. Similar results were observed for steady motions by Umavathi and Monica [40] in the absence of couple stress effects.

The linear solutions exhibit a considerable variety in behavior of the system, and the transition from linear to *nonlinear convection* can be quite complicated. It is necessary to study transient results in order to analyze nonlinear convective stability. The transition can be well understood by the analysis of equation (61) for which the solution gives a detailed description of the two-dimensional problem. The autonomous system of unsteady finite amplitude equations is solved numerically using the Runge-Kutta method. The Nusselt numbers are evaluated as functions of time *t*, the unsteady (transient) behavior of *NuT, NuF* and *NuC* is shown graphically in Figs. 7a-g, 8a-g and 9a-g respectively. These figures indicate that initially when time is small, there occur large scale oscillations in the values of Nusselt numbers indicating an unsteady rate of heat and mass transport in the fluid. As time passes, these values approach to the steady state corresponding to a near convection stage.
Figs. (7a, 8a, 9a), (7b, 8b, 9b), (7c, 8c, 9c) and (7d, 8d, 9d) depict the transient nature of thermal Nusselt number *NuT*, concentration Nusselt number *NuF* number and solute Nusselt number *NuC* with variation in nanoparticle concentration Rayleigh number *Rn*, nanofluid Lewis number *Ln*, modified diffusivity ratio N_A and on solutal Rayleigh number *Rs*. It is observed that as *Rn, Ln*, N_A and *Rs* increase, *NuT, NuF* and *NuC* are all enhanced, thus showing an increase in the heat and mass transport, which are the similar to trends observed by Agarwal *et al.* [23]. From Figs. (7d, 8d, 9d) we observe that viscosity ratio ν increases the heat and mass transport and in Figs. (7e, 8e, 9e) we observe that as conductivity ratio η increases the *NuT*, *NuF* and *NuC* decrease indicating that there is an inhibition of both heat and mass transports. Figs. 8f, 9f show that as the couple stress parameter C_P increases, the values of *NuF* and *NuC* also increase, thus showing an elevation in the heat and mass transport, while larger couple stress parameter C_P decreases the thermal Nusselt number *NuT*. Stronger non-Newtonian effect therefore reduces transfer of heat to the boundaries from the sandwiched layer with a concomitant cooling in the body of the layer. In the absence of couple stress parameter C_P all the results agree very well with earlier computations by Umavathi and Mohite [40].

5. Conclusions

A mathematical and numerical study of linear and nonlinear thermosolutal (double diffusive) convective instability in a horizontal porous medium saturated by a couple stress nanofluid, heated from below and cooled from above has been presented. The Darcy model for porous hydrodynamics has been deployed and nanoscale effects of Brownian motion and thermophoresis considered. Further the viscosity and thermal conductivity dependence on nanoparticle fraction have also been simulated by adopting the formulation of Tiwari and Das [33]. Linear analysis has been performed using the normal mode technique. However, for the nonlinear analysis, a truncated Fourier series representation having only two terms is considered. The following conclusions may be drawn:

1. Increasing Soret, Dufour, viscosity and thermal conductivity ratio parameters stabilize the system.
2. Increasing solutal Rayleigh number *Rs* destabilizes the system.
3. Increasing couple stresses stabilize the system for stationary and oscillatory convections.
4. The Nusselt, nanoparticle and solute concentrations are oscillatory for small time.
5. Steady state conditions are achieved for the Nusselt numbers when time is large.

Acknowledgements

The authors are grateful to all the reviewers for their comments which have served to improve the present manuscript.

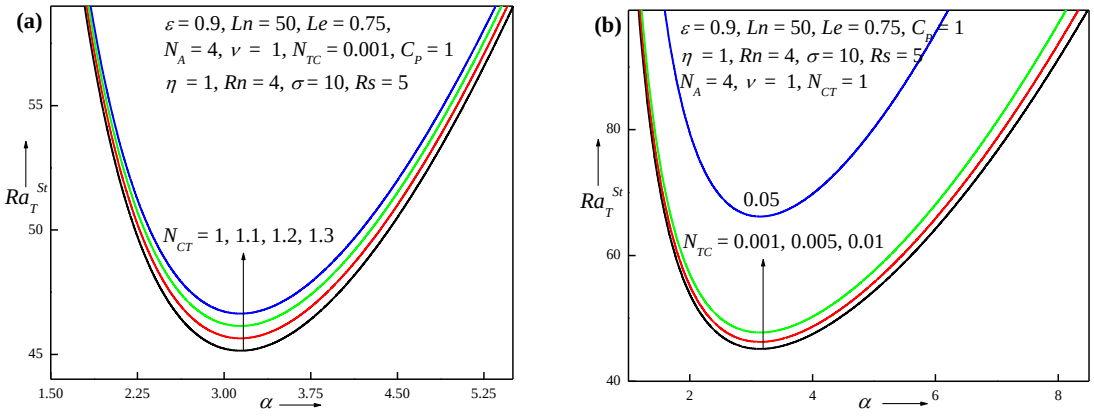

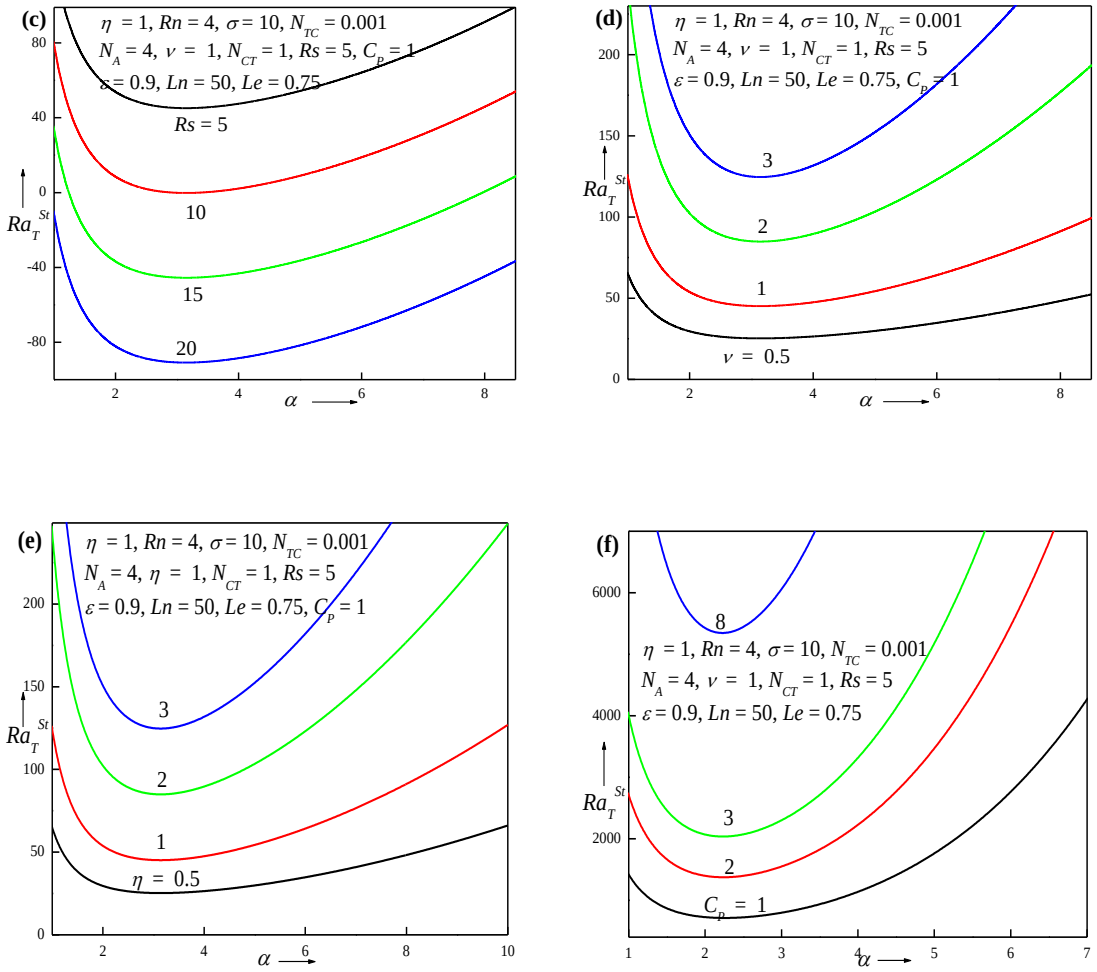

Figure 2. Neutral curves on stationary convection for different values of **(a)** Soret parameter N_{CT} **, (b)** Dufour parameter N_{TC} **, (c)** solutal Rayleigh number *Rs***,** **(d)**viscosity ratio ν **, (e)** thermal conductivity ratio η , **(f)** couple stress parameter C_P .

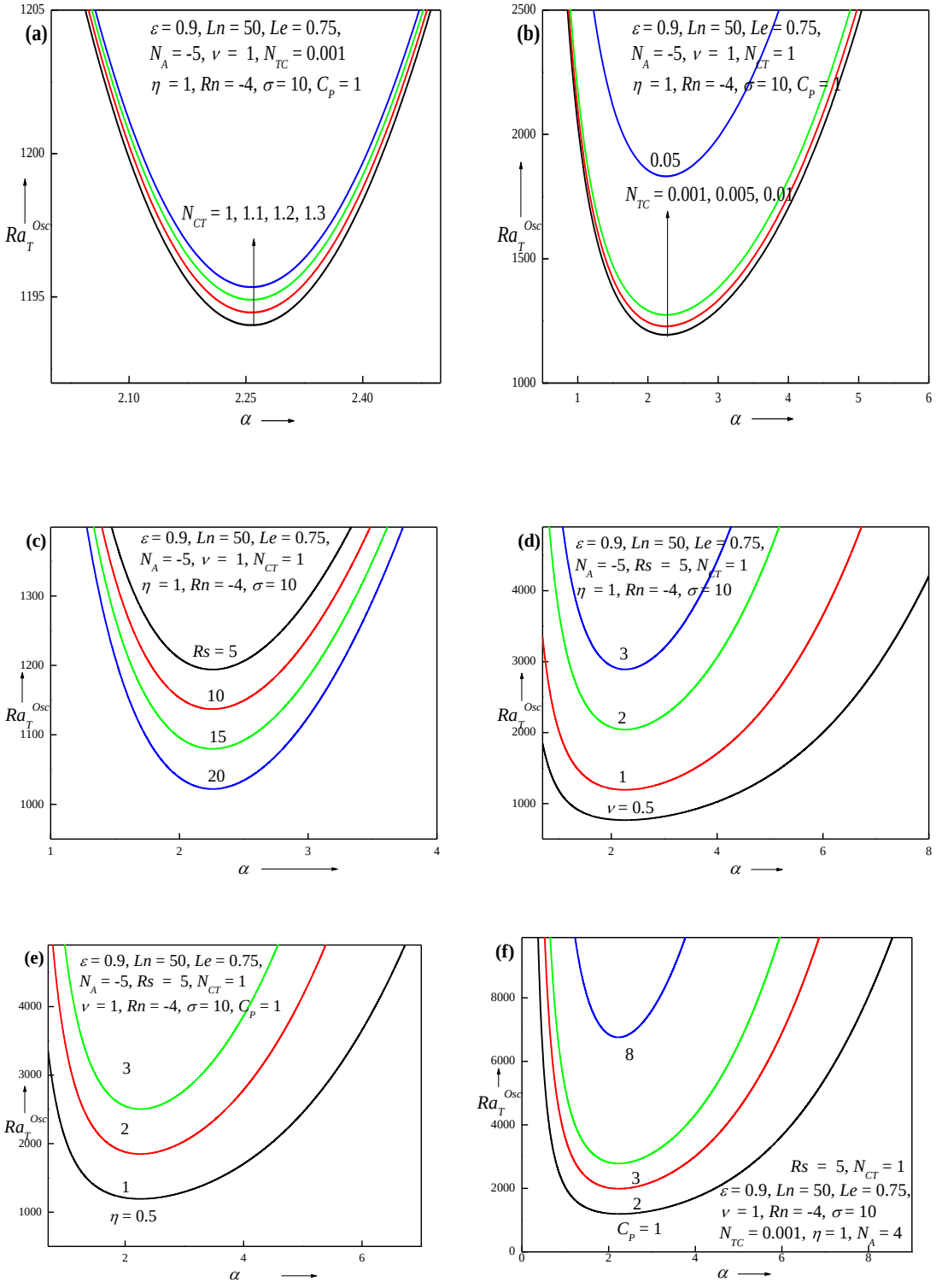

Figure 3. Neutral curves on oscillatory convection for different values of **(a)** Soret parameter N_{CT} **, (b)** Dufour parameter N_{TC} **, (c)** solutal Rayleigh number *Rs***,** **(d)**viscosity ratio ν **, (e)** thermal conductivity ratio η , **(f)** couple stress parameter C_P .

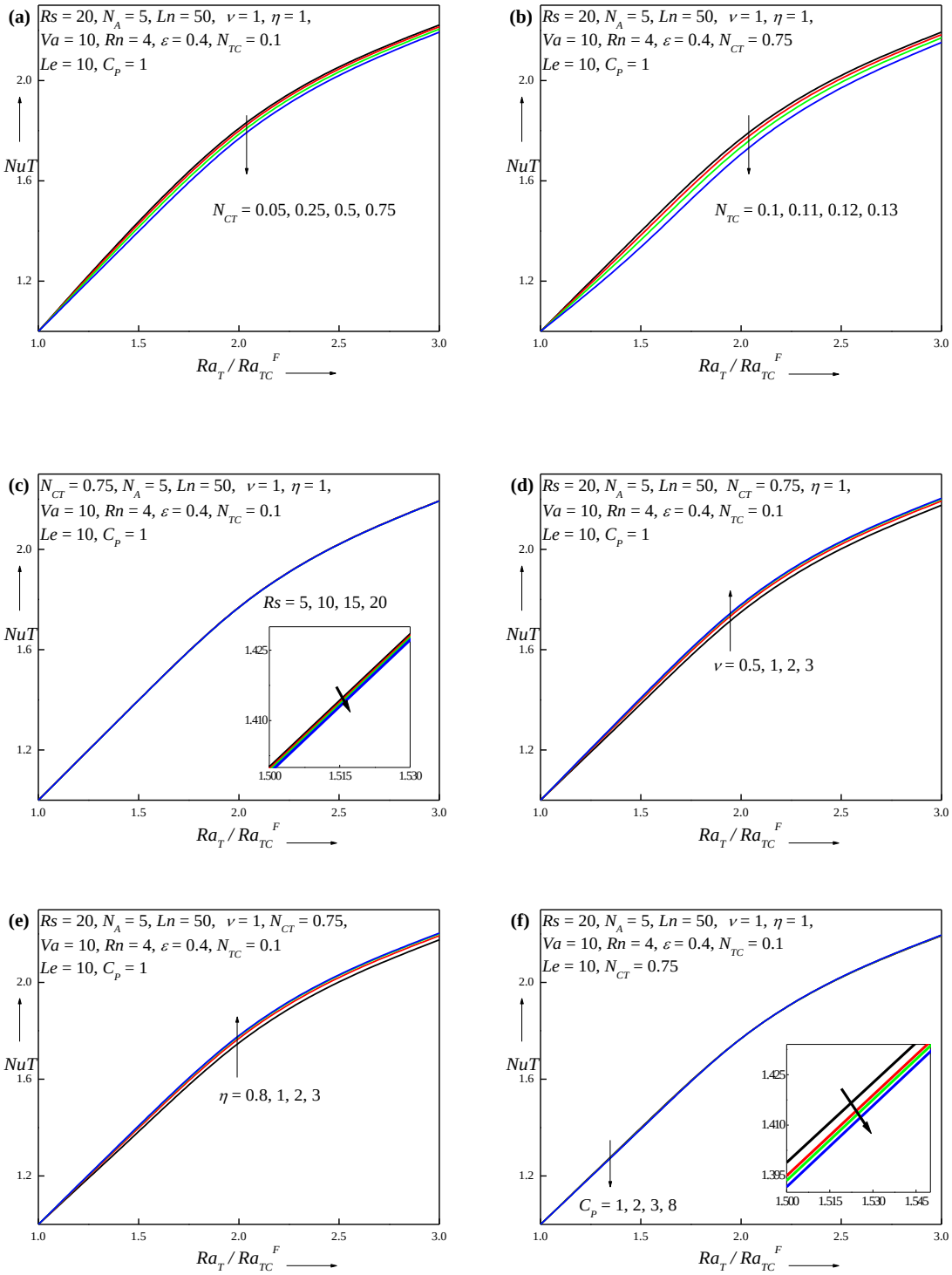

Figure 4. Variation of Thermal Nusselt number *NuT* with critical Rayleigh number for different values of **(a)** Soret parameter N_{CT} **, (b)** Dufour parameter N_{TC} **, (c)** solutal Rayleigh number *Rs***, (d)** viscosity ratio ν **, (e)** thermal conductivity ratio η , **(f)** couple stress parameter C_P .

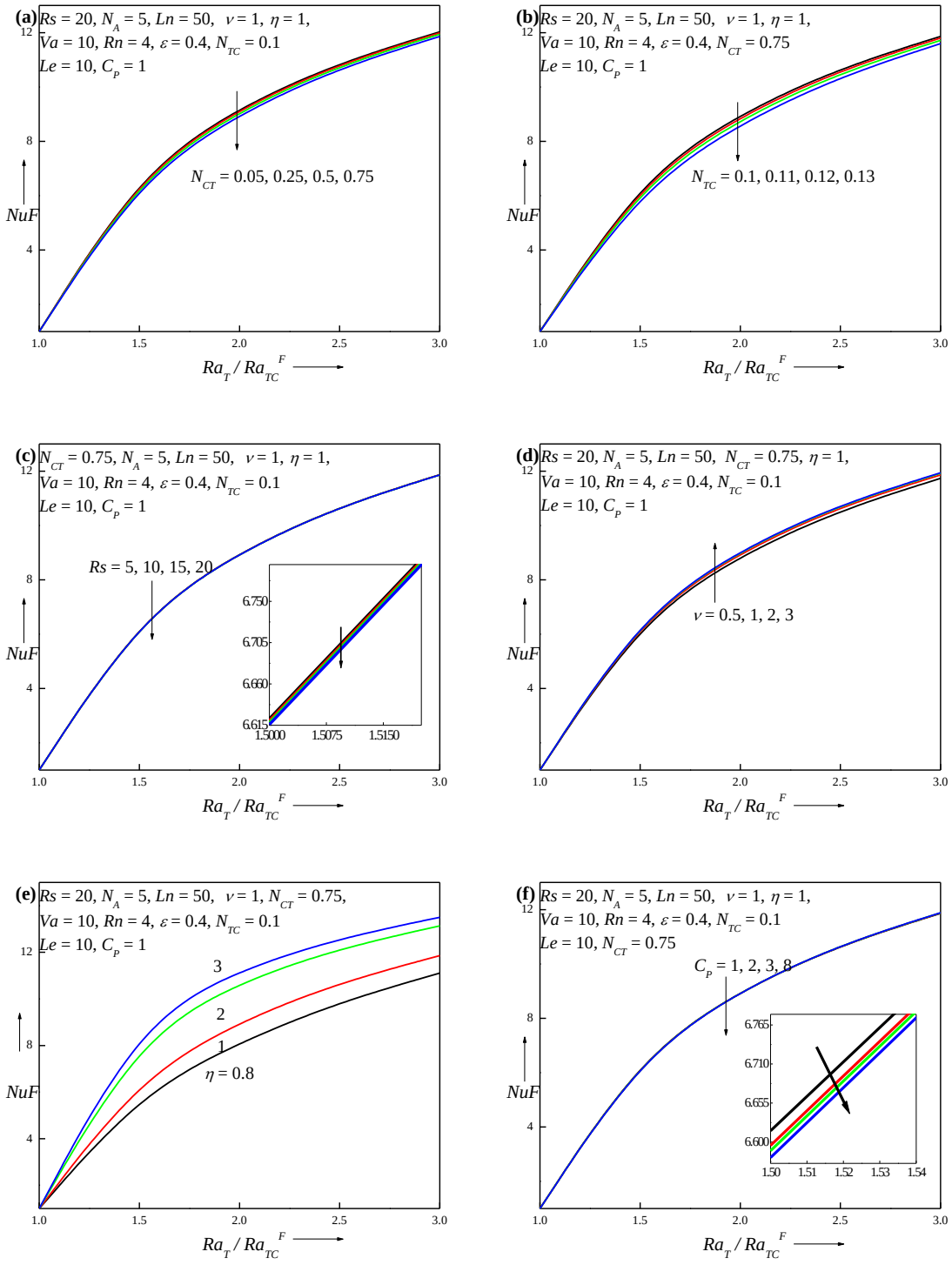

Figure 5. Variation of nanoparticle concentration Nusselt number *NuF* with critical Rayleigh number for different values of **(a)** Soret parameter N_{CT} **, (b)** Dufour parameter N_{TC} **, (c)** Solutal Rayleigh number *Rs***, (d)** viscosity ratio ν **, (e)** thermal conductivity ratio η , **(f)** couple stress parameter C_P .

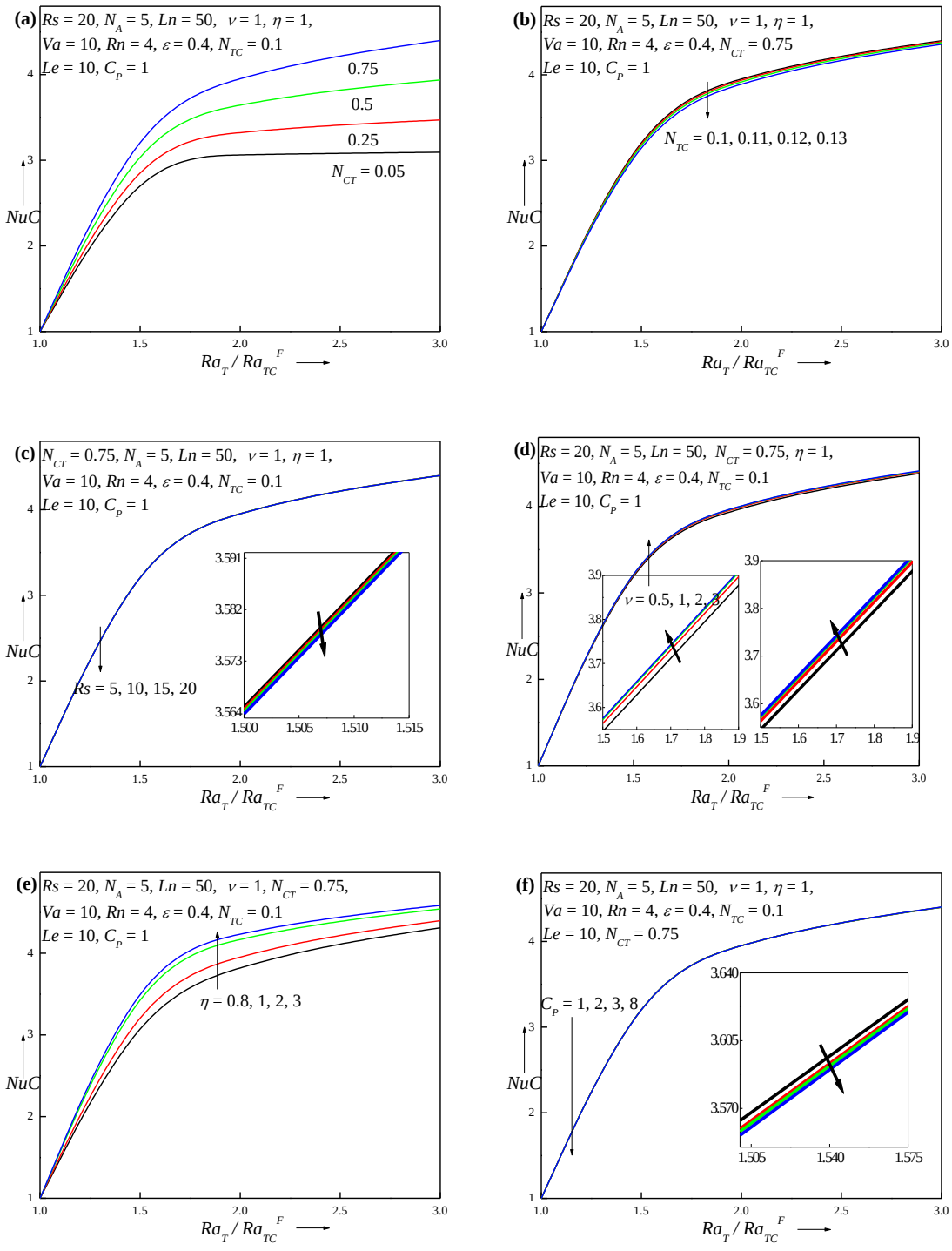

Figure 6. Variation of solute concentration Nusselt number *NuC* with critical Rayleigh Number for different values of **(a)** Soret parameter N_{CT} **, (b)** Dufour parameter N_{TC} **, (c)** solutal Rayleigh number *Rs***, (d)** viscosity ratio ν **, (e)** thermal conductivity ratio η , **(f)** couple stress parameter C_P .

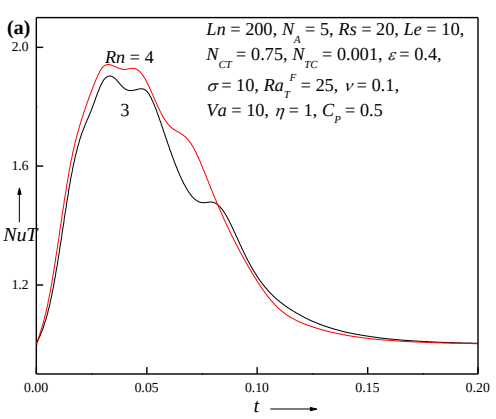
(a)
Ln = 200, N_A = 5, Rs = 20, Le = 10,
N_CT = 0.75, N_TC = 0.001, ε = 0.4,
σ = 10, Ra_T^F = 25, ν = 0.1,
Va = 10, η = 1, C_P = 0.5
Rn = 4
3
NuT
t

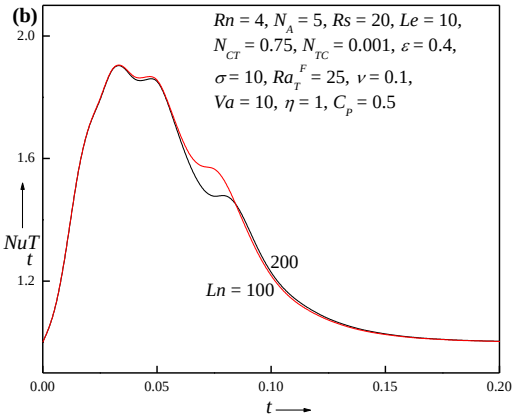
(b)
Rn = 4, N_A = 5, Rs = 20, Le = 10,
N_CT = 0.75, N_TC = 0.001, ε = 0.4,
σ = 10, Ra_T^F = 25, ν = 0.1,
Va = 10, η = 1, C_P = 0.5
200
Ln = 100
NuT
t

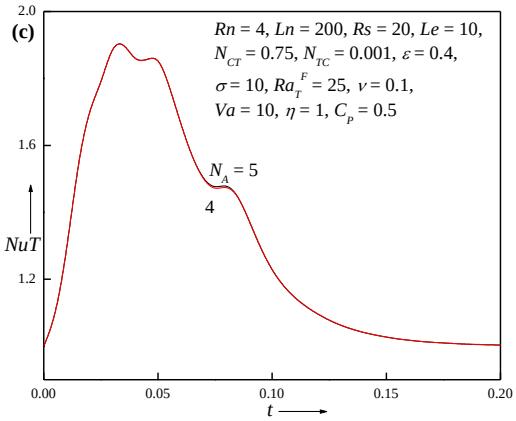
(c)
Rn = 4, Ln = 200, Rs = 20, Le = 10,
N_CT = 0.75, N_TC = 0.001, ε = 0.4,
σ = 10, Ra_T^F = 25, ν = 0.1,
Va = 10, η = 1, C_P = 0.5
N_A = 5
4
NuT
t

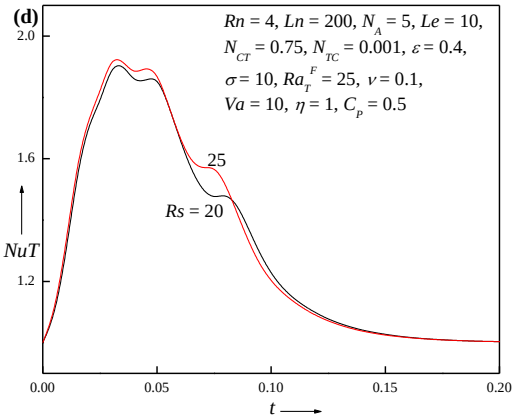
(d)
Rn = 4, Ln = 200, N_A = 5, Le = 10,
N_CT = 0.75, N_TC = 0.001, ε = 0.4,
σ = 10, Ra_T^F = 25, ν = 0.1,
Va = 10, η = 1, C_P = 0.5
25
Rs = 20
NuT
t

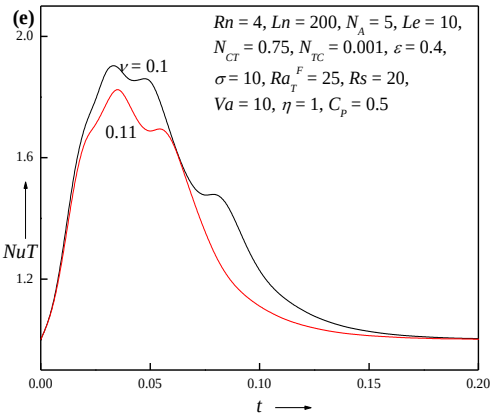
(e)
Rn = 4, Ln = 200, N_A = 5, Le = 10,
N_CT = 0.75, N_TC = 0.001, ε = 0.4,
σ = 10, Ra_T^F = 25, Rs = 20,
Va = 10, η = 1, C_P = 0.5
ν = 0.1
0.11
NuT
t

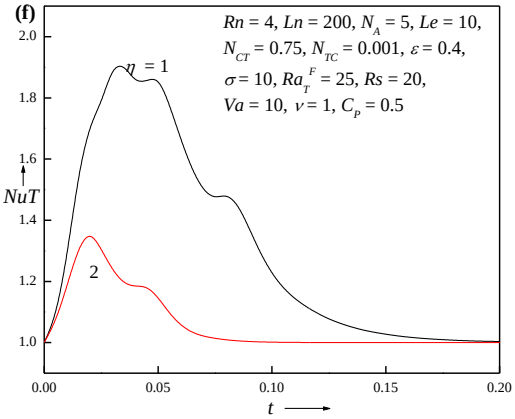
(f)
Rn = 4, Ln = 200, N_A = 5, Le = 10,
N_CT = 0.75, N_TC = 0.001, ε = 0.4,
σ = 10, Ra_T^F = 25, Rs = 20,
Va = 10, ν = 1, C_P = 0.5
η = 1
2
NuT
t

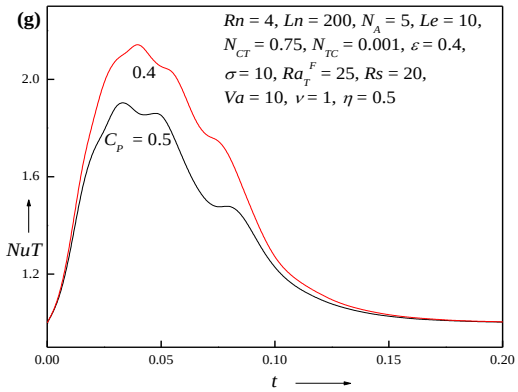

Figure 7. Transient thermal Nusselt number *NuT* versus time for different values of **(a)** Nanoparticle concentration Rayleigh number *Rn*, **(b)** Thermo-nanofluid Lewis number *Ln*, **(c)** Modified diffusivity ratio N_A, **(d)** Solutal Rayleigh number *Rs*, **(e)** Viscosity ratio ν, **(f)** Thermal conductivity ratio η, **(g)** couple stress parameter C_P.

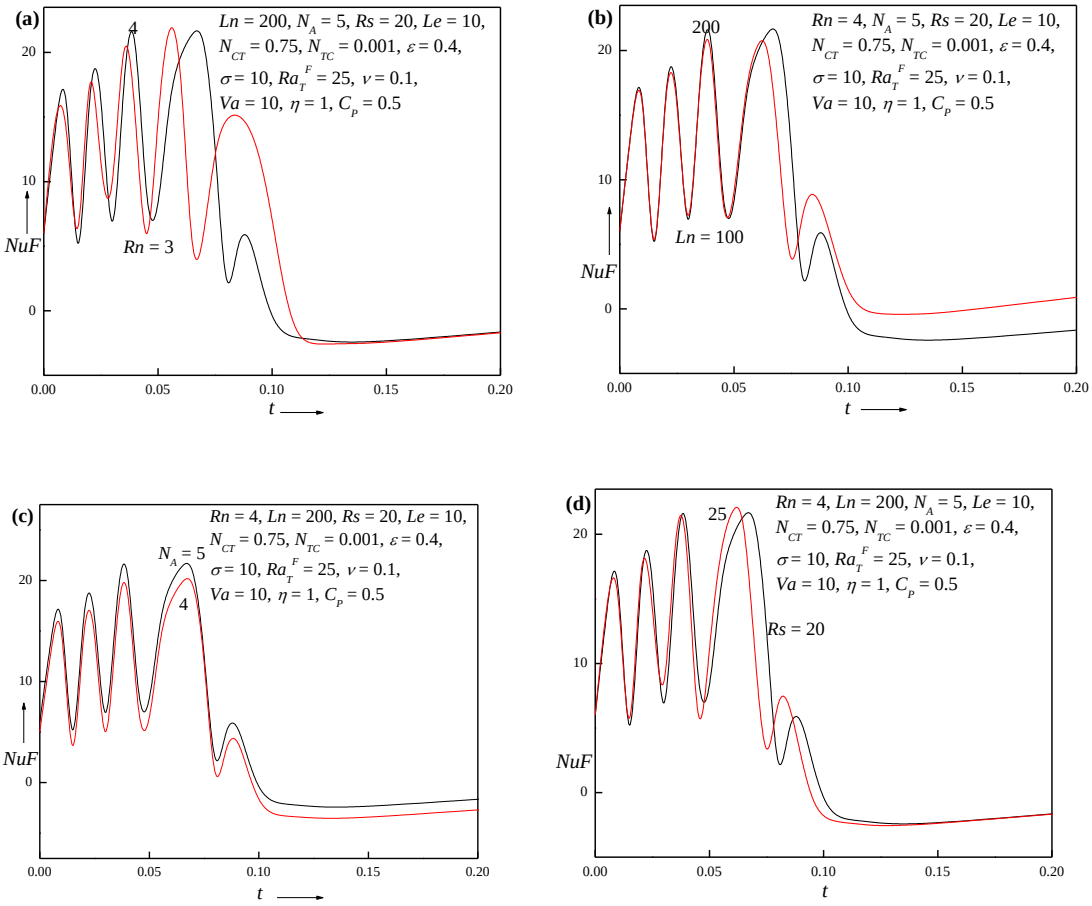

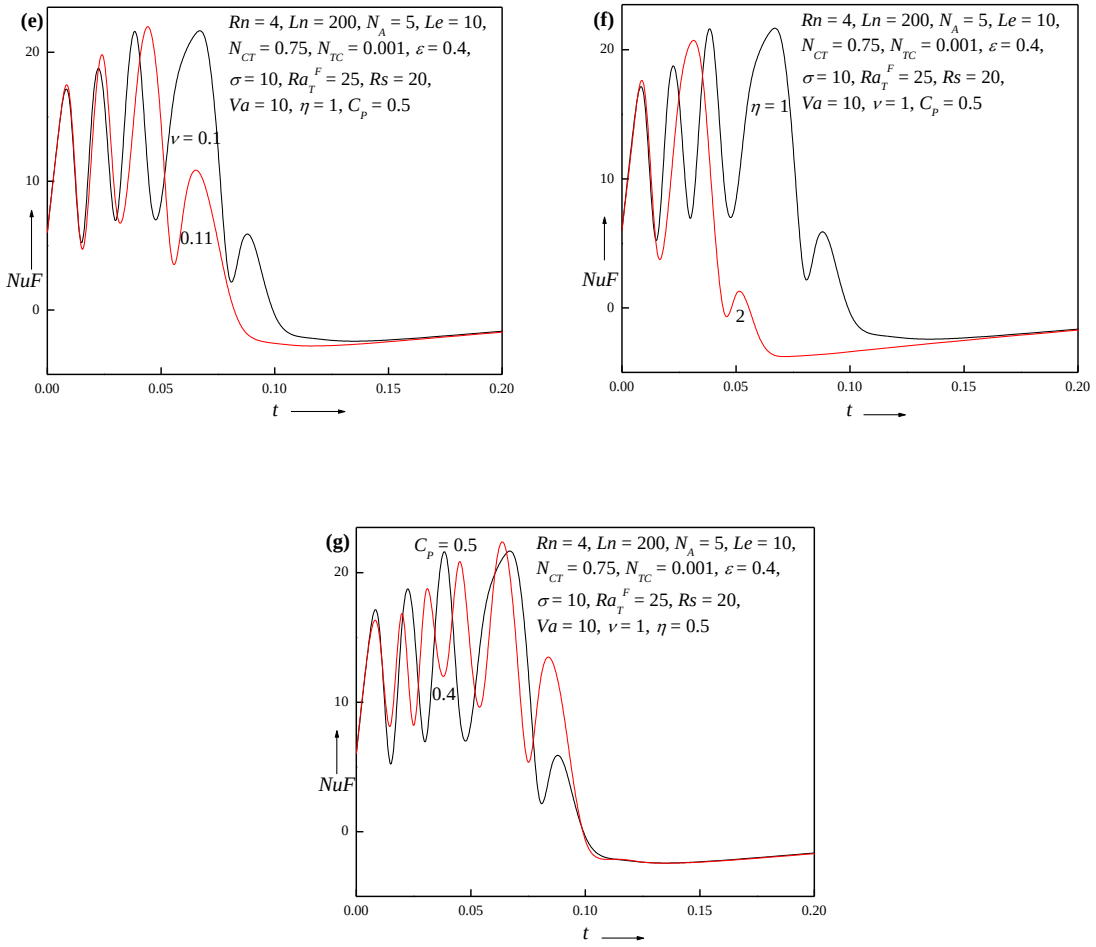

Figure 8. Transient nanoparticle concentration Nusselt number *NuF* with time for different values of **(a)** Nanoparticle concentration Rayleigh number *Rn*, **(b)** Thermo-nanofluid Lewis number *Ln*, **(c)** Modified diffusivity ratio N_A, **(d)** Solutal Rayleigh number *Rs*, **(e)** Viscosity ratio ν, **(f)** Conductivity ratio η, **(g)** Couple stress parameter C_P.

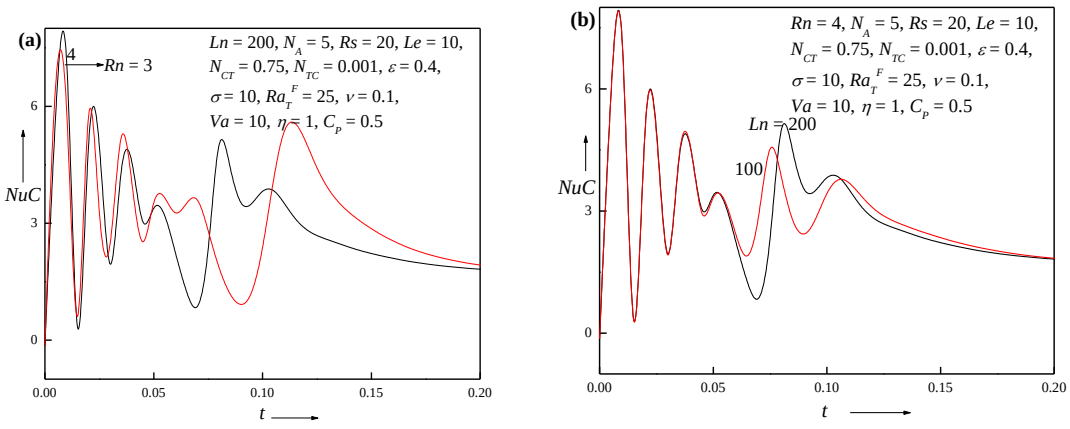

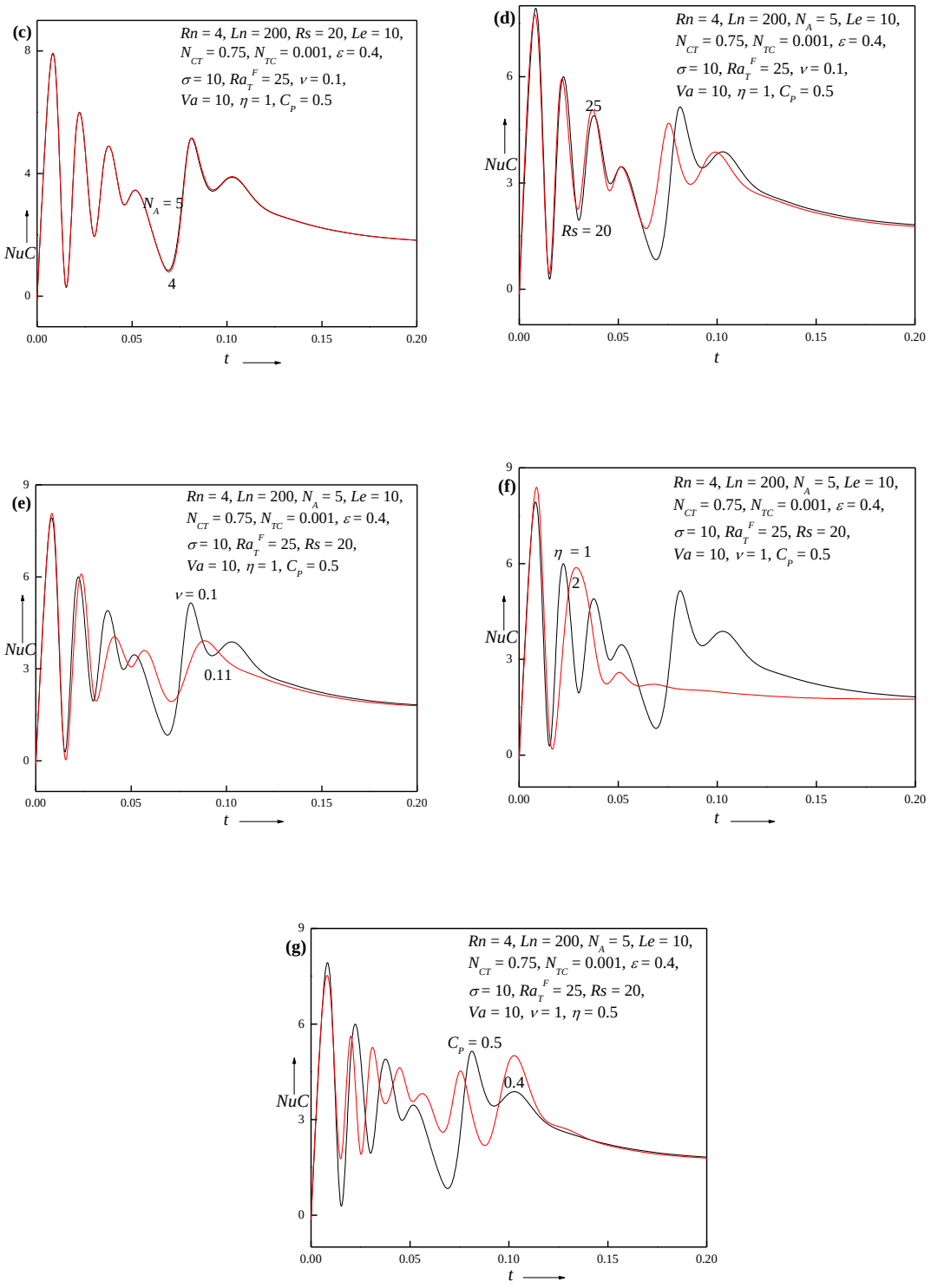

Figure 9. Transient solute concentration Nusselt number *NuC* versus time for different values of **(a)** Nanoparticle concentration Rayleigh number *Rn*, **(b)** Thermo-nanofluid Lewis number *Ln*, **(c)** Modified diffusivity ratio N_A, **(d)** Solutal Rayleigh number *Rs*, **(e)** Viscosity ratio ν, **(f)** Thermal conductivity ratio η, **(g)** Couple stress parameter C_P.

References

[1]. S.Ganguly, S. Sikdar, S. Basu, Experimental investigation of the effective electrical conductivity of aluminium oxide nanofluids, Powder Technol. 196 (2009) 326-330.

[2]. S. Merabia, S. Shenogin, L. Joly, P. Keblinski, J.L. Barrat, Heat transfer from nanoparticles: A corresponding state analysis, Proc. Natl. Acad. Sci. 106 (2009) 15113-15118.

[3]. S.U.S. Choi, J.A. Eastman, Enhancing thermal conductivity of fluids with nanoparticles, Proc. 1995 ASME Int. Mech. Eng. Congr. Expo. FED 231/MD. (1995) 99–105.

[4]. K.B. Anoop, S. Kabelac, T. Sundararajan, S.K. Das, Rheological and flow characteristics of nanofluids: Influence of electro viscous effects and particle agglomeration, J. Appl. Phys. 106 (2009) 034909.

[5]. S. Jain, H.E. Patel, S.K. Das, Brownian dynamic simulation for the prediction of effective thermal conductivity of nanofluid, J. Nanopart. Res. 11 (2009) 767-773.

[6]. R.S. Vajjha, D.K. Das, Specific heat measurement of three nanofluids and development of new correlations, ASME J. Heat Transfer. 131 (2009) 071601.

[7]. P.K. Namburu, D.P. Kulkarni, A. Dandekar, D.K. Das, Experimental investigation of viscosity and specific heat and silicon dioxide nanofluids, Micro Nano Lett. 2 (2007) 67-71.

[8]. S.Q. Zhou, R. Ni, Measurement of the specific heat capacity of water based Al_2O_3 nanofluid, Appl. Phys. Lett. 92 (2008) 093123-3.

[9]. S. Lee, S.U.S. Choi, S. Li, J.A. Eastman, Measuring thermal conductivity of fluids containing oxide nanoparticles, J. Heat Transf. 121 (1999) 280–289.

[10]. J. Buongiorno, Convective transport in nanofluids, J. Heat Transf. ASME 128 (2006) 240-250.

[11]. M. Sheikholeslami, A.J. Chamkha, P. Rana, R. Moradi, Combined thermophoresis and Brownian motion effects on nanofluid free convection heat transfer in an L-shaped enclosure, Chinese Journal of Physics. 55 (2017) 2356-2370.

[12]. M.F.M. Basir, E.H. Hafidzuddin, K. Naganthran, Hashim, S.S. Chaharborj, M.S.M. Kasihmuddin, R. Nazar, Stability analysis of unsteady stagnation-point gyrotactic bioconvection flow and heat transfer towards the moving sheet in a nanofluid, Chinese

Journal of Physics. 65 (2020) 538-553.

[13]. M. Sheikholeslami, B. Rezaeianjouybari, M. Darzi, A. Shafee, Z. Li, T.K. Nguyen, Application of nano-refrigerant for boiling heat transfer enhancement employing an experimental study, Int. J. of Heat and Mass Transfer. 141 (2019) 974–980.

[14]. M. Sheikholeslami, R. Haq, A. Shafee, Z. Li, Y.G. Elaraki, I. Tlili, Heat transfer simulation of heat storage unit with nanoparticles and fins through a heat exchanger, Int. J. Heat Mass Transfer. 135 (2019) 470–478.

[15]. M. Sheikholeslami, M. Jafaryar, A. Shafee, H. Babazadeh, Acceleration of discharge process of clean energy storage unit with insertion of porous foam considering nanoparticle enhanced paraffin, Journal of Cleaner Production. 261 (2020) 121206.

[16]. M. Sheikholeslami, M. Jafaryarb, E. Abohamzehc, A. Shafeed, H. Babazadehe, Energy and entropy evaluation and two-phase simulation of nanoparticles within a solar unit with impose of new turbulator, Sustainable Energy Technologies and Assessments. 39 (2020) 100727

[17]. T. Mahalakshmi, N. Nithyadevi, H.F. Oztop, N. Abu-Hamdeh, Natural convective heat transfer of Ag-water nanofuid flow inside enclosure with center heater and bottom heat source, Chinese Journal of Physics. 56 (2018) 1497-1507.

[18]. I. Waini, A. Ishak, I. Pop, Unsteady flow and heat transfer past a stretching/shrinking sheet in a hybrid nanofluid, Int. J. Heat Mass Transf. 136 (2019) 288–297.

[19]. I. Waini, A. Ishak, I. Pop, Flow and heat transfer of a hybrid nanofluid past a permeable moving surface, Chinese Journal of Physics. 66 (2020) 606-619.

[20]. M. Izadia, M.A. Sheremet, S.A.M. Mehryanc, Natural convection of a hybrid nanofluid affected by an inclined periodic magnetic field within a porous medium, Chinese Journal of Physics. 65 (2020) 447–458.

[21]. D.A. Nield, A. Bejan, Convection in Porous Media, 3rd edn, New York, Springer, 2006.

[22]. A. Mojtabi, M.C. Charrier-Mojtabi, Double-diffusive convection in porous media Handbook of Porous Media (Ed.) K. Vafai, New York: Dekker, 2000, 559–603.

[23]. A. Mojtabi, M.C. Charrier-Mojtabi, Double-diffusive convection in porous media Handbook of Porous Media 2nd Handbook of Porous Media (Ed.) K. Vafai, New York, Taylor and Francis, 2005, 269–32.

[24]. M. Mamou, Stability analysis of double–diffusive convection in porous enclosures Transport Phenomena in Porous Media II Eds., D B Ingham and I Pop, Oxford: Elsevier,

2002, 113–54.

[25]. S. Kumar, S. Ghosh, B. Samet, E.F.D. Goufo, An analysis for heat equations arises in diffusion process using new Yang-Abdel-Aty-Cattani fractional operator, Math. Meth. Appl. Sci. (2020) 1–19.

[26]. S. Kumar, R. Kumar, R.P. Agarwal, B. Samet, A study of fractional Lotka-Volterra population model using Haar wavelet and Adams-Bashforth-Moulton methods, Math. Meth. Appl. Sci. (2020) 1–15.

[27]. J.C. Umavathi, S. Mohiuddin, M.A. Sheremet, MHD flow in a vertical channel under the effect of temperature dependent physical parameters, Chinese Journal of Physics. 58 (2019) 324–338.

[28]. D.A. Nield, Onset of thermohaline convection in a porous medium, Water Resour. Res. 4 (1968) 553–560.

[29]. J.W. Taunton, E.N. Lightfoot, T. Green, Thermohaline instability and salt fingers in a porous medium, Phys. Fluids. 15 (1972) 748–753.

[30]. R.C. Sharma, K.D. Thakur, On couple stress fluid heated from below in porous medium in hydrodynamics, Czech. J. Phys. 50 (2000) 753–758.

[31]. Sunil, R.C. Sharma, R.S. Chandel, On superposed couple stress fluids in porous medium in hydromagnetics, Z. Naturforsch. A 57 (2002) 955–960.

[32]. Sunil, R.S.Sharma, R.S. Chandel, Effect of suspended particles on couple stress fluid heated and soluted from below in porous medium, J. Porous Media 7 (2004) 9–18.

[33]. R.K. Tiwari, M.K. Das, Heat transfer augmentation in a two-sided lid-driven differentially heated square cavity utilizing nanofluids, Int. J. Heat Mass Transf. 50 (2007) 2002–2018.

[34]. H.C. Brinkman, The viscosity of concentrated suspensions and solutions, J. Chem. Physics. 20 (1952)571-581.

[35]. J.C. Maxwell, A Treatise on Electricity and Magnetism, 2nd edn. Oxford University Press, UK 1904.

[36]. D.A. Nield, General heterogeneity effects on the onset of convection in a porous

medium. In: Vadász, P. (ed.) Emerging Topics in Heat and Mass Transfer in Porous Media. 63–84. Springer. New York 2008.

[37]. S. Agarwal, B.S. Bhadauria, N.C. Sacheti, P. Chandran, A.K. Singh, Non-linear convective transport in a binary nanofluid saturated porous layer, Transp. Porous Media. 93 (2012) 29–49.

[38]. M.S. Malashetty, M.S. Swamy, W. Sidram, Double diffusive convection in a rotating anisotropic porous layer saturated with viscoelastic fluid, Int. J. Thermal Sciences (2011) 1757-1769.

[39]. B.S. Bhadauria, S. Agarwal, Natural convection in a nanofluid saturated rotating porous layer: A nonlinear study, Transp. Porous Media 87 (2011) 585–602.

[40]. J.C. Umavathi, B.M. Monica, Double-diffusive convective transport in a nanofluid-saturated porous layer with cross diffusion and variation of viscosity and conductivity, Heat Transfer—Asian Research 43 (2014) 628-652.